NASA Technical Paper 1234

Modal Control Theory and Application to Aircraft Lateral Handling Qualities Design

S. Srinathkumar

JUNE 1978

NASA

NASA Technical Paper 1234

Modal Control Theory and Application to Aircraft Lateral Handling Qualities Design

S. Srinathkumar
Langley Research Center
Hampton, Virginia

National Aeronautics
and Space Administration

**Scientific and Technical
Information Office**

1978

SUMMARY

A multivariable synthesis procedure based on eigenvalue/eigenvector assignment is reviewed and is employed to develop a systematic design procedure to meet the lateral handling qualities design objectives of a fighter aircraft over a wide range of flight conditions. The study reveals that the closed-loop modal characterization developed provides significant insight into the design process and plays a pivotal role in the synthesis of robust feedback systems. The simplicity of the synthesis algorithm yields an efficient computer-aided interactive design tool for flight control system synthesis.

INTRODUCTION

It has been recognized that for flight control system design, state space-oriented procedures provide significant design advantages over classical control design using root locus, Bode, and Nyquist techniques. If the aircraft model is represented in the state space framework, two well-known synthesis procedures are the linear quadratic regulator design and pole-placing technique. The quadratic synthesis procedure is particularly well suited to those systems which have desired response time histories as performance specification. However, aircraft handling qualities design objectives originate in the frequency domain as desirable locations of closed-loop poles (eigenvalues in state variable representation) with satisfactory damping characteristics.

A major difficulty encountered in the quadratic regulator formulation is selection of appropriate optimal performance indices to meet desired handling qualities. This difficulty has been partially resolved by characterizing the quadratic performance indices in terms of asymptotic eigenvalues and eigenvectors. (See ref. 1.) This study (ref. 1) confirms that the modal control formulation is an appropriate synthesis framework for aircraft handling qualities design.

The synthesis of multivariable systems based on pole-placement criteria has developed into several well-documented procedures (refs. 2 to 4) but none have proved to be effective design procedures. The common difficulty is not the fault of the algorithms but is really due to the inherent inability of pole (eigenvalue) specifications to characterize the actual variable responses. The state feedback law assigning a specified set of eigenvalues is not unique for multi-input systems. Different laws yield identical eigenvalues but radically different eigenvectors. Further, an eigenvector determines the influence of the corresponding eigenvalue on the state variable response. Thus, control of the modal matrix (matrix of eigenvectors) structure becomes as essential as satisfying eigenvalue specifications in order to effectively shape the dynamic response of the feedback system.

Based on this key concept, it is possible to formulate the multivariable synthesis problem as an eigenvalue/eigenvector assignment problem. (See

ref. 5.) This new formulation reveals that for an n-state, m-input system, up to m entries in each closed-loop eigenvector can be arbitrarily chosen, in addition to assigning all n eigenvalues. Thus, the eigenvector selection freedom can be successfully used for response shaping.

The purpose of this report is to establish systematic synthesis procedures for the selection of eigenvalues and eigenvectors to meet a wide variety of performance requirements. In particular, the eigenvalue/eigenvector modification process is illustrated. Control laws for a typical fighter aircraft are synthesized to improve Dutch roll damping, turn coordination, and sideslip gust response over a wide range of flight conditions.

SYMBOLS

Values are given in SI and U.S. Units where appropriate. Any consistent set of units may be used elsewhere.

A	system matrix
a, a_i	scalars defined in equations (A1) and (A5)
a_y	lateral acceleration, m/sec^2 (ft/sec^2)
B	input matrix
b, b_i	scalars defined in equations (A1) and (A5)
$C, \bar{C}$	measurement matrices defined in equations (29) and (B1)
C_i, C_k	matrices defined in equations (10) and (17)
$D, \bar{D}$	matrices defined in equations (29) and (B1)
d_{ij}	scalar defined after equation (23)
e_r	vector defined in notation (1) of "Spectral Synthesis Algorithm"
F	matrix defined in equation (8)
$f_r^{(k-1)}$	vector defined in step 4(a) of algorithm
G	matrix defined in equation (8)
g	acceleration due to gravity, 9.8 m/sec^2 (32.2 ft/sec^2)
$g_r^{(k)}$	vector defined in step 4(a) of algorithm
H	matrix defined in equation (33)
$h_r^{(k-1)}$	vector defined in step 4(a) of algorithm

I_{index}	(index)th order identity matrix
i,j	indices
$K, \hat{K}, \tilde{K}$	feedback matrices
k_{A_j}	feedback from jth variable to aileron channel, $j = p, \dot{\psi}, \beta, a_y, \phi$
k_{R_j}	feedback from jth variable to rudder channel, $j = p, \dot{\psi}, \beta, a_y, \phi$
k_{R_A}	aileron to rudder interconnect gain
L	elementary permutation matrix defined in observation 4 following algorithm description
$L'_p, L'_r, L'_\beta, L'_{\delta_a}, L'_{\delta_r}$	aircraft derivatives defined after equation (29)
$M_p, M_r, M_\beta, M_\phi, M_{\delta_a}, M_{\delta_r}$	aircraft derivatives defined after equation (29)
$M^{(k)}$	matrix defined in equation (16)
m	number of inputs
$m_a^{(k)}, m_b^{(k)}$	vectors defined after equation (16)
N	matrix of eigenvectors defined prior to equation (15)
$N'_p, N'_r, N'_\beta, N'_{\delta_a}, N'_{\delta_r}$	aircraft derivatives defined after equation (29)
n	number of states
P	matrix defined after equation (31)
p	roll rate, deg/sec
$Q^{(k-1)}$	matrix defined in notation (6) of algorithm
q	vector defined in equation (A1)
$R^{(k-1)}$	matrix defined immediately before equation (15)
$r \in \{\Delta^{(k)}\}$	r is an element of the set $\Delta^{(k)}$
S	matrix defined in equation (8)
s	vector defined in equation (A1)
t_i	vector defined in equation (21)
t	time index
u	input vector defined in equation (1)

u_p input vector defined in equation (2)

V modal matrix (matrix of eigenvectors)

V_0 total equilibrium velocity, m/sec (ft/sec)

v_i, v_j, v_k eigenvectors

w_i, w_{i+1} vectors used in equations (8) and (A5); a partition of v_i, v_{i+1}

x state vector defined by equation (1)

$x \in R^n$ $n \times 1$ real vector x

$Y_p, Y_r, Y_\beta, Y_{\delta_a}, Y_{\delta_r}$ aircraft derivatives defined in equation (29)

$y, \bar{y}$ output vectors defined after equations (29) and (B1), respectively

z_i, z_{i+1} vectors used in equations (8) and (A5); a partition of v_i, v_{i+1}

$\alpha_1, \alpha_2, \alpha_3, \alpha_i$ scalars defined in numerical example 1

β sideslip, deg

$\Delta(1), \Delta(k)$ set of indices defined in notation (5) of "Spectral Synthesis Algorithm"

δ scalar

$\delta_1, \delta_2, \delta_3$ matrix elements used in equation (14)

δ_A pilot aileron input

δ_R pilot rudder input

δ_a aileron angular deflection, deg

δ_r rudder angular deflection, deg

$\delta\lambda_k, \delta z_k$ perturbed quantities defined in step 2 and step 5 of algorithm

ε scalar

$\varepsilon_1, \varepsilon_2, \varepsilon_3$ matrix elements used in equation (14)

ζ_d Dutch roll mode damping factor

θ sideslip parameter defined in quantitative aircraft performance specification

Λ diagonal matrix of eigenvalues

λ_i, λ_k eigenvalues

π_i mode condition number defined in equation (25)

ρ 2 × 2 matrix defined in equation (A4)

Σ_k 2 × 2 matrix defined in observation 1 following algorithm description

σ_k scalar defined by notation (4) of algorithm

τ_R roll subsidence time constant

ϕ bank angle, deg

$\dot{\psi}$ yaw rate, deg/sec

ω_{nd} Dutch roll mode natural frequency

Superscripts:

T matrix transpose

-1 matrix inverse

^,- transformed quantity

Notations:

$\| \ \|$ matrix or vector norm

$\| \ \|_2$ Euclidian norm

$| \ |$ absolute value

$>>$ far greater than

$\approx$ approximately

$\prod$ continued product used in observation 4 following algorithm

Upper case letters of the alphabet denote matrices; matrix subscripts indicate partitioned quantities. A dot over a quantity denotes a derivative with respect to time.

SPECTRAL CHARACTERIZATION

The concept of rationally utilizing the freedom in control law selection to satisfy eigenvalue as well as eigenvector specifications forms a useful basis for the development of multivariable synthesis algorithms. Unfortunately, the

process of coupling the effect of the individual modes (eigenvalues) to the state variable responses through the eigenvector entries is nonlinear. This fact becomes apparent if the state variable response is derived by using the modal canonical form. However, it is possible to identify certain desired closed-loop system structures and consequently associated modal structures. For example, it is often the case that higher order systems may be considered as a coupling of lower order subsystems, each with its own specifications of acceptable performance. In such a case, the eigenvectors should be selected so that the eigenvalues appropriate to one set of response variables do not unduly influence the other responses. Similarly, it may be desirable to segregate short-time constant variables from long-time constant modes or to insure that systems with both real and complex pair poles have eigenvectors selected so that minimal oscillatory behavior will arise in those responses associated with real eigenvalues.

The eigenvectors may, of course, be modified without disturbing pole locations through the nonuniqueness of the modal control process. There is also insufficient freedom to completely select the individual eigenvector shapes. Thus, the general synthesis approach will be to structure the design process so that maximum capabilities are achieved for satisfying whatever eigenvalue/eigenvector specifications exist. The multivariable synthesis problem will now be formulated as an eigenvalue/eigenvector selection problem as follows.

Consider the controllable system

$$\dot{x} = Ax + Bu \tag{1}$$

where $x \in R^n$, $u \in R^m$, and A and B are properly dimensioned. Assume that B is full rank. The state variable feedback law takes the form

$$u = Kx + u_p \tag{2}$$

where K is the feedback matrix and u_p is an external reference input. The problem is to select a K so that the closed-loop system matrix $A + BK$ satisfies

$$[A + BK]v_i = \lambda_i v_i \qquad (i = 1,2,\ldots,n) \tag{3}$$

where λ_i is the ith eigenvalue and v_i is the corresponding eigenvector.

The formulation given by equation (3) permits a certain freedom in the choice of the eigenvector elements. In order to identify which of the eigenvector elements can be arbitrarily chosen, partition equation (3) as

$$\left\{\begin{bmatrix} A_{11} & \cdots & A_{12} \\ \vdots & & \vdots \\ A_{21} & \cdots & A_{22} \end{bmatrix} + \begin{bmatrix} B_1 \\ \vdots \\ B_2 \end{bmatrix} \begin{bmatrix} K_1 : K_2 \end{bmatrix}\right\} \begin{bmatrix} z_i \\ \vdots \\ w_i \end{bmatrix} = \lambda_i \begin{bmatrix} z_i \\ \vdots \\ w_i \end{bmatrix} \qquad (i = 1,2,\ldots,n) \qquad (4)$$

where A_{11}, B_1, and K_1 are $m \times m$ matrices and other matrices are compatibly dimensioned. Also, assume that B_1 is nonsingular (if necessary by at most reordering the state variables). z_i is an $m \times 1$ vector, z_i and w_i are partitions of the eigenvector v_i, and $v_i^T = \left[z_i^T : w_i^T\right]$. Completing the multiplication of the partitioned quantities yields

$$\left[A_{11} + B_1K_1\right] z_i + \left[A_{12} + B_1K_2\right] w_i = \lambda_i z_i \qquad (5)$$

$$\left[A_{21} + B_2K_1\right] z_i + \left[A_{22} + B_2K_2\right] w_i = \lambda_i w_i \qquad (6)$$

From equation (5), it follows that

$$K_1z_i + K_2w_i = B_1^{-1}\left[\lambda_i z_i - A_{11}z_i - A_{12}w_i\right] \qquad (7)$$

Substituting $K_1z_i + K_2w_i$ from equation (7) into equation (6) yields the following fundamental eigenvector constraining relationship

$$\left[\lambda_i I_{n-m} - F\right] w_i = \left[G + \lambda_i S\right] z_i \qquad (i = 1,2,\ldots,n) \qquad (8)$$

where I_{n-m} is an $(n - m)$th order identity matrix and S, G, and F are matrices defined by

$$\left.\begin{aligned} S &= B_2B_1^{-1} \\ G &= A_{21} - SA_{11} \\ F &= A_{22} - SA_{12} \end{aligned}\right\} \qquad (9)$$

Appendix A develops relations similar to equation (8) for complex pair eigenvalue computations using real arithmetic. Now equation (8) constitutes a set

of $n - m$ linear equations in the n unknown elements of each eigenvector. Thus, if λ_i is not an eigenvalue of F, at most m elements corresponding to the z_i vector can be arbitrarily chosen. Then the remaining $n - m$ eigenvector elements corresponding to the w_i vector can be computed from equation (8) as

$$w_i = C_i z_i \qquad (i = 1,2,\ldots,n) \tag{10}$$

where $C_i = \left[\lambda_i I_{n-m} - F\right]^{-1}\left[G + \lambda_i S\right]$ is defined as the "modal coupling matrix" corresponding to λ_i.

The preceding analysis shows that all n eigenvalues and up to $n \cdot m$ eigenvector elements can be arbitrarily assigned through the use of state variable feedback. The resulting modal matrix

$$V = \left[v_1 : v_2 : \ldots : v_n\right]$$

however, must be nonsingular.

It is also important to note that equation (8) shows the complete relationship between the eigenvalues and associated eigenvectors. This relationship not only illustrates the eigenvector forms that can be achieved by state feedback, but it also points out immediately that certain preconceived objectives may be impossible to achieve. Later examples illustrate this point.

Hence, the design approach is complete in the sense that when it fails to satisfy certain specifications, it does so by showing that no state feedback control law could satisfy them. Thus, the analysis provides a complete spectral characterization of all closed-loop realizations given the triple (A,B,λ_i).

It should also be noted that the free $n \cdot m$ elements of the modal matrix V (z_i-vectors) correspond exactly to the $n \cdot m$ arbitrary elements of the feedback matrix K. This establishes the parametric equivalence between the nonunique feedback matrix K and the arbitrary modal entries.

With a nonsingular modal matrix V and eigenvalue matrix Λ chosen subject to the constraints of equation (8), the closed-loop system matrix $\hat{A} = A + BK$ is uniquely determined by

$$\hat{A} = \begin{bmatrix} \hat{A}_{11} & \cdots & \hat{A}_{12} \\ \vdots & & \vdots \\ \hat{A}_{21} & \cdots & \hat{A}_{22} \end{bmatrix} = V\Lambda V^{-1} \tag{11}$$

The required feedback matrix K which yields this closed-loop matrix $\hat{A}$ can be easily computed by using the relations

$$\left.\begin{aligned} K_1 &= B_1^{-1}\left[\hat{A}_{11} - A_{11}\right] \\ K_2 &= B_1^{-1}\left[\hat{A}_{12} - A_{12}\right] \end{aligned}\right\} \tag{12}$$

The preceding analysis relies on the generation of a nonsingular transformation V (modal matrix). It is possible to prove the existence of a nonsingular modal matrix for any specified Λ (ref. 6). However, this proof imposes an unduly restricted structure on the modal matrix. This result is in contrast to a practical synthesis perspective where the designer may well be willing to accept a modest perturbation in a pole location if this will allow significant gains in flexibility of selection of eigenvector entries. This is particularly true if the designer will have control of the perturbation size and therefore will be able to control stability properties. This design philosophy has led to the development of the algorithm to be presented in the section entitled "Spectral Synthesis Algorithm." This algorithm consistently strives to satisfy both eigenvalue and eigenvector specifications while allowing the user to control the perturbations in the design criteria.

The concepts of the modal control process will now be illustrated with two numerical examples. The first example illustrates the eigenvalue/eigenvector selection procedure. The second example motivates the need for the development of a systematic algorithmic procedure to insure the generation of a nonsingular modal matrix.

NUMERICAL EXAMPLES

Example 1

The following problem is presented to describe the synthesis procedure and indicates the trade-offs between design specifications and achievable results may be required. Suppose that the plant dynamics are

$$\begin{bmatrix} \dot{x}_1 \\ \dot{x}_2 \\ \dot{x}_3 \end{bmatrix} = \begin{bmatrix} 1 & 1 & -1 \\ 0 & 3 & -2 \\ 1 & 1 & -1 \end{bmatrix} \begin{bmatrix} x_1 \\ x_2 \\ x_3 \end{bmatrix} + \begin{bmatrix} 1 & 0 \\ 0 & 1 \\ 0 & 0 \end{bmatrix} \begin{bmatrix} u_1 \\ u_2 \end{bmatrix} \tag{13}$$

and the control law

$$\begin{bmatrix} u_1 \\ u_2 \end{bmatrix} = K \begin{bmatrix} x_1 \\ x_2 \\ x_3 \end{bmatrix}$$

is to be selected so that

(1) Pole locations are at $\lambda_1 \approx -100$, $\lambda_2 \approx -10$, and $\lambda_3 \approx -1$.

(2) The variables x_1, x_2, and x_3 should exhibit, respectively, the short-, intermediate-, and long-time constant transients, namely, 0.01, 0.1, and 1 second, respectively.

(3) The responses should be decoupled in the sense that although x_3 may exhibit short and intermediate transients, e^{-t} will rapidly dominate other terms, x_2 should not have e^{-t} terms, and x_1 should exhibit neither e^{-t} nor e^{-10t} transients.

Note that this is not a trivial problem since the open-loop system eigenvalues are at 0, 1, and 2 and the crucial long-time constant is to be associated with x_3, the variable not directly influenced by the input.

The time solution for the closed-loop system in terms of the modal matrix V can be expressed as

$$x(t) = V \exp(\Lambda t) V^{-1} x(0)$$

or in terms of the individual components as

$$\begin{bmatrix} x_1(t) \\ x_2(t) \\ x_3(t) \end{bmatrix} = \begin{bmatrix} v_{11} & v_{12} & v_{13} \\ v_{21} & v_{22} & v_{23} \\ v_{31} & v_{32} & v_{33} \end{bmatrix} \begin{bmatrix} \alpha_1 e^{\lambda_1 t} \\ \alpha_2 e^{\lambda_2 t} \\ \alpha_3 e^{\lambda_3 t} \end{bmatrix}$$

where the α_i terms depend on V^{-1} and the initial conditions $x(0)$, and $\lambda_1 \approx -100$, $\lambda_2 \approx -10$, and $\lambda_3 \approx -1$. Although the entries of the modal matrix influence the α_i terms in a nonlinear fashion, dominance arguments show that the design specifications will be satisfied if V is of the form

$$V = \begin{bmatrix} v_{11} & \varepsilon_1 & \varepsilon_2 \\ \delta_1 & v_{22} & \varepsilon_3 \\ \delta_2 & \delta_3 & v_{33} \end{bmatrix} \tag{14}$$

where the ε and δ values should be small compared with v_{ii} $(i = 1,2,3)$. This procedure will yield minimal cross coupling and preserve the diagonal dominance character of V^{-1}.

To begin the synthesis, denote each column of V by v_j, and

$$v_j = \begin{bmatrix} z_{1j} \\ z_{2j} \\ \cdot \cdot \cdot \\ w_{1j} \end{bmatrix}$$

For the system represented by equation (13), the respective matrices of equation (8) are

$$S = 0$$

$$F = -1$$

$$G = \begin{bmatrix} 1 & 1 \end{bmatrix}$$

By requiring $\Lambda = \text{Diag}\ (-100,-10,-1)$ and starting with $j = 3$ ($\lambda_3 = -1$ is the most crucial eigenvalue), the procedure is to select z_{13}, z_{23}, and λ_3 and evaluate w_{13} from

$$w_{13} = \frac{z_{13} + z_{23}}{\lambda_3 + 1}$$

This is seen to be a "best case" problem (at least thus far); since λ_3 may be selected as exactly -1, both z_{13} and z_{23} selected to be zero, and $w_{13} = 1$.

It should be noted that the eigenvalue selected coincides with the matrix F. This coincident eigenvalue selection will be discussed further in the spectral synthesis algorithm description. Thus,

$$v_3 = \begin{bmatrix} 0 \\ 0 \\ 1 \end{bmatrix}$$

For $j = 2$,

$$w_{12} = \frac{z_{12} + z_{22}}{\lambda_2 + 1}$$

where z_{12} and w_{12} (corresponding to ϵ_1 and δ_3 in eq. (14)) should be small compared with z_{22}, and λ_2 should be about -10. For numerical simplicity, select $\lambda_2 = -11$, $z_{22} = 1$, $z_{12} = 0$, and w_{12} is then found to be -0.1. Note that this selection of eigenvector entries is not "best case," since w_{12} and z_{12} cannot be both zero if z_{22} is to be nonzero. This implies there must be some coupling of the system modes. By continuing the synthesis,

$$v_2 = \begin{bmatrix} 0 \\ 1 \\ -0.1 \end{bmatrix}$$

It is seen by inspection that the two eigenvectors are independent. However, a higher dimension problem will require an algorithmic procedure to insure the linear independence of the eigenvectors.

For $j = 1$,

$$w_{11} = \frac{z_{11} + z_{21}}{\lambda_1 + 1}$$

and for selecting $\lambda_1 = -101$, it is desired that z_{11} dominate both w_{11} and z_{21}. Clearly, both conditions cannot be satisfied (again implying some coupling is unavoidable). But by selecting $z_{11} = 1$ and $z_{21} = -1$, w_{11} will be zero and the inverse of V will preserve the diagonally dominant structure. Again,

$$v_1 = \begin{bmatrix} 1 \\ -1 \\ 0 \end{bmatrix}$$

is clearly linearly independent of v_2 and v_3 by inspection. The modal matrix V has now been found to be

$$V = \begin{bmatrix} 1 & 0 & 0 \\ -1 & 1 & 0 \\ 0 & -0.1 & 1 \end{bmatrix}$$

with the inverse

$$V^{-1} = \begin{bmatrix} 1 & 0 & 0 \\ 1 & 1 & 0 \\ 0.1 & 0.1 & 1 \end{bmatrix}$$

The closed-loop system matrix is found to be

$$\hat{A} = V\Lambda V^{-1}$$

$$\hat{A} = \begin{bmatrix} -101 & 0 & 0 \\ 90 & -11 & 0 \\ 1 & 1 & -1 \end{bmatrix}$$

Thus, the required feedback gains are easily calculated from equations (12) as

$$K = \begin{bmatrix} -102 & -1 & 1 \\ 90 & -14 & 2 \end{bmatrix}$$

The time response of the system is given by

$$\begin{bmatrix} x_1(t) \\ x_2(t) \\ x_3(t) \end{bmatrix} = V \exp[\Lambda t] V^{-1} \begin{bmatrix} x_{10} \\ x_{20} \\ x_{30} \end{bmatrix}$$

Thus,

$$x_1(t) = x_{10}\, e^{-101t}$$

$$x_2(t) = -x_{10}\, e^{-101t} + (x_{10} + x_{20}) e^{-11t}$$

$$x_3(t) = -0.1(x_{10} + x_{20}) e^{-11t} + (0.1x_{10} + 0.1x_{20} + x_{30}) e^{-t}$$

It is seen that the performance specifications have been achieved and that the only coupling is from transients which rapidly become dominated by the desired time constant solutions. It is again emphasized that the example is "best case," since the ability to select four identically zero entries in the modal matrix insured the total unidirectional coupling. To now consider a "worst case" example, suppose the problem were the same except that

$$A = \begin{bmatrix} 1 & 1 & -1 \\ 0 & 3 & -2 \\ 1 & 1 & 19 \end{bmatrix}$$

where only the element a_{33} in the A matrix has been changed.

The first step of the solution is to again select $\lambda_3 \approx -1$, with

$$w_{13} = \frac{z_{13} + z_{23}}{\lambda_3 - 19}$$

and $|w_{13}| \gg |z_{13}|$ and $|w_{13}| \gg |z_{23}|$. These conditions certainly cannot even be approximately satisfied; thus, any solution will exhibit considerable mode coupling.

One particular compromise solution yielded a modal matrix

$$V = \begin{bmatrix} -1 & 0 & -10 \\ 0 & -1 & 0 \\ 0.05 & 0.033 & 0.1 \end{bmatrix}$$

with $\Lambda = \text{Diag}\,[-1, -11, -81]$, and the corresponding state variable responses

$$x_1(t) = (0.167x_{10} - 0.555x_{20} - 16.667x_{30})e^{-t} + 10(0.083x_{10} + 0.056x_{20} + 1.667x_{30})e^{-81t}$$

$$x_2(t) = x_{20}\, e^{-11t}$$

$$x_3(t) = 0.05(-0.167x_{10} + 0.555x_{20} + 16.667x_{30})e^{-t} - 0.03x_{20}\, e^{-11t} + 0.1(0.083x_{10} + 0.056x_{20} + 1.667x_{30})e^{-81t}$$

The following observations may be made about this particular solution:

(1) The solution for $x_1(t)$ is the only one which does not meet specifications.

(2) If $x_1(t)$ were a more important variable than $x_2(t)$, selection of modal matrix entries could be made to have $x_1(t)$ free of cross-coupled transients (e^{-t}, e^{-10t}), but this would introduce an e^{-t} transient in the $x_2(t)$ response.

To summarize, the proposed technique yields desirable results in "best case" examples, and for "worst case" problems provides at the least a forewarning of the type of mode couplings that will occur. Also, in less tractable problems the displaying of the system closed-loop modal structure shows that no other solution will yield the desirable response. These discussions also demonstrate the inevitable trade-off involved in any synthesis procedure and highlight the need to recognize fully the physical constraints of the plant, as exhibited by the modal coupling matrices C_i (eq. (10)) to evolve acceptable design goals.

Example 2

A simple numerical example is now presented to highlight the final basis for the establishment of the design algorithm to be presented in the next

section. It will illustrate that certain procedural idiosyncrasies, as simple as selecting the sequence of synthesizing eigenvectors, may induce problems which could be resolved by inspection for low order systems, but do require an algorithmic process for more complex systems.

Suppose the plant dynamics are given by

$$\begin{bmatrix} \dot{x}_1 \\ \dot{x}_2 \\ \dot{x}_3 \end{bmatrix} = \begin{bmatrix} 1 & 0 & 0 \\ 1 & 5 & 6 \\ -1 & -1 & 0 \end{bmatrix} \begin{bmatrix} x_1 \\ x_2 \\ x_3 \end{bmatrix} + \begin{bmatrix} 1 & 0 \\ 0 & 1 \\ 0 & 0 \end{bmatrix} \begin{bmatrix} u_1 \\ u_2 \end{bmatrix}$$

with open-loop eigenvalues at 1, 2, and 3. Suppose further that design specifications are $\lambda_1 = -1$, $\lambda_2 = -2$, $\lambda_3 = -1$, and an eigenvector structure

$$V = \begin{bmatrix} 1 & -1 & -1 \\ 0 & 1 & 1 \\ w_1 & w_2 & w_3 \end{bmatrix}$$

with the w elements computed to meet the desired pole specifications.

To complete the design, equation (8) can be used immediately (where $F = 0$, $S = 0$, and $G = \begin{bmatrix} -1 & -1 \end{bmatrix}$) to yield

$$v_1 = \begin{bmatrix} 1 \\ 0 \\ 1 \end{bmatrix}$$

$$v_2 = \begin{bmatrix} -1 \\ 1 \\ 0 \end{bmatrix}$$

$$v_3 = \begin{bmatrix} -1 \\ 1 \\ 0 \end{bmatrix}$$

It is immediately obvious that the resulting modal matrix V will be singular, since v_2 and v_3 are identical. For a third-order problem such as this, equation (8) may be examined directly for each eigenvalue, and a sound decision made as to which specifications should be relaxed and in what manner to give a system performance very close to that desired. Of course, for substantially higher order systems or for an automated on-line controller, a precisely defined algorithm is required. Such an algorithm is now presented, and this problem is reexamined as an illustration of its utility.

SPECTRAL SYNTHESIS ALGORITHM

As the discussions in the previous sections revealed, the central question in the new formulation of the pole-placement problem is the guaranteed generation of the nonsingular matrix V satisfying equation (8). An examination of the eigenvector constraints shows that there is an m-dimensional subspace associated with each eigenvalue. Thus, the problem reduces to selecting a nonsingular set of n eigenvectors with each vector included from a subspace associated with a particular eigenvalue. However, this method is an inefficient way to synthesize since the designer loses direct control of the selection of arbitrary elements of the modal matrix (z-vectors). Also, any algorithm would become computationally intractable since it would involve pairing n vectors from a set of $n \cdot m$ vectors until a nonsingular set resulted.

Alternatively, if the z-vectors are allowed to be chosen arbitrarily, then it is important to keep track of the linear independence of the eigenvectors as they are sequentially generated. Unfortunately, this procedure is potentially susceptible to the generation of a singular set of eigenvectors since it is very likely that no closed-loop matrix with the precise set of eigenvalues and eigenvectors as selected would exist for any choice of control law. This is exactly what occurred in example 2 of the section entitled "Numerical Examples." However, is it possible to detect the occurrence of such a situation by selecting the eigenvectors sequentially as follows.

Let $N = \left[v_1 : v_2 : \ldots : v_{k-1}\right]$ be the matrix of $k-1$ linearly independent eigenvectors already generated. Then the projector of the subspace spanning these eigenvectors is given by

$$R^{(k-1)} = N\left[N^T N\right]^{-1} N^T$$

Selecting the kth eigenvector v_k so that

$$R^{(k-1)} v_k \neq v_k \tag{15}$$

insures the linear independence of the kth eigenvector. In the numerical example 2, equation (15) cannot be satisfied for the third eigenvalue and eigenvector specification. This condition implies a slight perturbation in the

eigenvalue and/or eigenvector specification must be made to insure the linear independence of the eigenvectors.

An algorithm is now presented which incorporates the condition of equation (15) without having to compute the projection matrices $R^{(k-1)}$ explicitly. The sequential synthesis of the eigenvectors is accomplished in a special canonical form in which the testing of the linear independence between the eigenvectors is straightforward. Further, the procedure allows the designer to insure the linear independence between the synthesized eigenvectors to a degree determined by a prespecified tolerance parameter. For clarity of presentation, the algorithm is detailed for real eigenvalues. The extension to complex conjugate pairs follows as a natural extension of the real eigenvalue problem.

The following notations are used throughout the algorithm presentation:

(1) e_r is an n-vector with rth entry equal to unity and all other entries zero.

(2) $v_k^T = \left[z_k^T : w_k^T\right]$ is the kth eigenvector, where z_k is the designer specified m-vector.

(3) $v_k^{(k-1)} = Q^{(k-1)} v_k$ where $Q^{(0)} = I_n$ and $Q^{(i)}$, $i \neq 0$, will be defined in notation (6).

(4) $v_{rk}^{(k-1)}$ is the rth element of $v_k^{(k-1)}$ and for convenience of notation $v_{rk}^{(k-1)} = \sigma_k$.

(5) $M^{(k)}$ is an $n \times n$ matrix of the form

$$M^{(k)} = \begin{bmatrix} & \vdots & & \vdots & \\ I_{n-r} & \vdots & m_a^{(k)} & \vdots & 0 \\ \cdots & \cdots & \cdots & \cdots & \cdots \\ & \vdots & & \vdots & \\ 0 & \vdots & 1 & \vdots & 0 \\ & \vdots & & \vdots & \\ \cdots & \cdots & \cdots & \cdots & \cdots \\ & \vdots & & \vdots & \\ 0 & \vdots & m_b^{(k)} & \vdots & I_{r-1} \end{bmatrix} \tag{16}$$

where the vectors $m_a^{(k)}$ and $m_b^{(k)}$ are computed so that the vector $v_k^{(k-1)}$ is transformed to a canonical form as

$$M^{(k)} v_k^{(k-1)} = \sigma_k e_r; \quad r \in \left\{\Delta^{(k)}\right\}$$

where $\Delta^{(k)}$ is a subset of integers $\{1,2,\ldots,n\}$ containing the indices not already used in the construction of the matrices $M^{(1)}$, $M^{(2)}$, . . ., $M^{(k-1)}$,

and $\Delta^{(1)}$ is the complete set $\{1,2,\ldots,n\}$. Note $M^{(k)}$ can be constructed, if and only if, $\sigma_k \neq 0$.

(6) $Q^{(k-1)} = M^{(k-1)}M^{(k-2)} \ldots M^{(1)}$ $\qquad (k > 1)$

The algorithm now proceeds as follows:

Step 1: For $k = 1,2,\ldots,n$, do steps 2 to 5.

Step 2: For $\lambda = \lambda_k$, compute $\det\left[\lambda_k I_{n-m} - F\right]$.

(a) If $\det = 0$, perturb λ_k to $(\lambda_k + \delta\lambda_k)$ and repeat step 2.

(b) If $\det \neq 0$, go to step 3.

Step 3: For $\lambda = \lambda_k$, compute C_k (eq. (10)) as

$$C_k = \left[\lambda_k I_{n-m} - F\right]^{-1}\left[G + \lambda_k S\right] \tag{17}$$

Step 4: For some $r \in \left\{\Delta^{(k)}\right\}$

(a) Compute the m-vector

$$\left[g_r{}^{(k)}\right]^T = f_r{}^{(k-1)} + h_r{}^{(k-1)}C_k$$

where $\left(f_r{}^{(k-1)} : h_r{}^{(k-1)}\right)$ is the rth row of the transformation $Q^{(k-1)}$ (notation (6)) and $h_r{}^{(k-1)}$ is a $(n - m)$-row vector.

(b) Compute

$$\sigma_k = \left[g_r{}^{(k)}\right]^T z_k \tag{18}$$

where z_k is the arbitrarily specified m design vector.

(i) If $\sigma_k \neq 0$, compute w_k (eq. (10)) and $M^{(k)}$ (eq. (16)) and go to step 1.

(ii) If $\sigma_k = 0$, select another $r \in \left\{\Delta^{(k)}\right\}$ and return to step 4(a).

(iii) If $\sigma_k = 0$ for all $r \in \left\{\Delta^{(k)}\right\}$, go to step 5.

Step 5: For some $r \in \left\{\Delta^{(k)}\right\}$

(a) If $g_r{}^{(k)} \neq 0$, perturb z_k to $(z_k + \delta z_k)$ to make $\sigma_k \neq 0$ (eq. (18)), compute w_k and $M^{(k)}$, and go to step 1.

(b) If $g_r^{(k)} = 0$, select another $r \in \{\Delta^{(k)}\}$ and repeat step 5(a).

(c) If $g_r^{(k)} = 0$, all $r \in \{\Delta^{(k)}\}$, perturb λ_k to $(\lambda_k + \delta\lambda_k)$ and go to step 2.

Step 6: Compute the feedback gains by using equations (12).

Step 7: Stop.

The kth linearly independent eigenvector v_k can be synthesized provided $\sigma_k \neq 0$. This can be seen clearly as follows. Without loss of generality, let the first $(k - 1)$ eigenvectors be generated with indices $r = 1,2,\ldots,(k - 1)$. Then these vectors are transformed into a canonical form under $Q^{(k-1)}$ as

$$Q^{(k-1)}\left[v_1 : v_2 : \ldots : v_{k-1}\right] = \left[\begin{array}{c} \text{Diag}\left[\sigma_1,\sigma_2,\ldots,\sigma_{k-1}\right] \\ \hline 0 \end{array}\right]$$

with

$$\sigma_i \neq 0 \qquad (i = 1,2,\ldots,k - 1)$$

and the projector spanning the subspace of these transformed eigenvectors has the simple form

$$R^{(k-1)} = \begin{bmatrix} I_{k-1} & \cdot & 0 \\ & \cdot & \\ \cdots & \cdots & \cdots \\ & \cdot & \\ 0 & \cdot & 0 \end{bmatrix}$$

Now choosing the kth eigenvector so that its transformed vector becomes $v_k^{(k-1)} = Q^{(k-1)}v_k$ causes

$$\sigma_k \neq 0 \qquad \left(r \in \{k,k+1,\ldots,n\}\right)$$

and insures the linear independence of v_k since the constraint (eq. (15)) is clearly satisfied.

The following observations can be made regarding the algorithm outlined:

(1) The algorithm can be directly extended to complex pairs in quasi-diagonal form as described. Two eigenvectors are synthesized in one iteration

and equation (A5) is used instead of equation (8). Further, the test condition $\sigma_k \neq 0$ in step 4(b(i)) is modified to testing the nonsingularity of a 2×2 matrix Γ_k. This matrix is constructed by selecting two rows of the transformation matrix $Q^{(k-1)}$ obtained in the previous iteration and developing a condition similar to equation (18). The transformation matrix $M^{(k)}$ for the complex pair is then obtained as a product of two transformations corresponding to the real eigenvectors $[v_k : v_{k+1}]$ associated with ρ_k. This procedure will insure the linear independence between v_k and v_{k+1}.

(2) Explicit evaluation of the eigenvalues of matrix F is not needed to detect coincident mode assignment. It is sufficient to determine the appropriate determinant in step 2, this determinant being available as a byproduct in the synthesis of the kth eigenvector when C_k is evaluated. If a mode is coincident with the spectrum of F, then a perturbation of the mode is required to insure $[\lambda_k I_{n-m} - F]$ is nonsingular and hence that equation (8) has a solution for any arbitrary z_k. The degree of perturbation needed depends on the numerical tolerance set on the evaluation of the determinant. Also since the eigenvalue shift in step 2 is a designer's choice, system stability is always insured. Alternatively, if the eigenvalue assigned coincides with the spectrum of F, special eigenvector structures can be derived by noting that equation (8) has a solution for $z_i = 0$, and also for $[G + \lambda_i S]z_i = 0$ if $(n - m) < m$. (See ref. 6.)

(3) The iterative procedure in step 4(b(ii)) attempts to meet exact eigenvalue/eigenvector specifications. In step 5(b) an attempt is made to meet exact eigenvalue specifications with slightly relaxed eigenvector specifications (z-vector). The test in step 5(c) indicates that the eigenvalue specification implies that the corresponding eigenvector will lie in the eigensubspace already synthesized; this condition demands a perturbation in the eigenvalue specification.

(4) Since the matrices $M^{(k)}$ have only one nontrivial column, coordinate transformations $Q^{(k-1)}$ reduce to simple vector multiplications. Further, the inverse of V required in equation (10) to evaluate the feedback gains in equations (12) is easily evaluated by noting that $Q^{(n)}V$ has the general form

$$Q^{(n)}V = \text{Diag}\left[\sigma_1, \sigma_2, \ldots, \sigma_n\right]L$$

The matrix L is an elementary permutation matrix dependent on the sequence of generating the indices $r \in \left\langle \Delta^{(k)} \right\rangle$ in steps 4 and 5, the σ_k are the nonzero pivotal elements, and

$$V^{-1} = L^{-1}\,\text{Diag}\left[\frac{1}{\sigma_1}, \frac{1}{\sigma_2}, \ldots, \frac{1}{\sigma_n}\right]Q^{(n)}$$

Also notice that

$$\left|\det\left[V\right]\right| = \left|\prod_{k=1}^{n} \sigma_k\right|$$

since $\left|\det\left[Q^{(n)}\right]\right|$ and $\left|\det\left[L\right]\right|$ are unity.

Thus, the numbers σ_i provide a good measure of the linear independence between the eigenvectors provided the eigenvector entries are scaled to a standard basis as $v_i^T v_i = 1$ for example. Thus, the numerical ill-conditioning of the modal matrix V for inversion is controlled by setting a tolerance on σ_k $(k = 1,2,\ldots,n)$ to pass the test $\sigma_k \neq 0$. The important bearing of this modal matrix numerical condition on system sensitivity properties is discussed in the section entitled "Modal Sensitivity Analysis."

(5) A noteworthy feature of the algorithm is that the eigenvectors do not explicitly undergo any change in the sequence of transformations $Q^{(k-1)}$; thus, the mode coupling characteristics of C_k are kept transparent during synthesis, a very desirable feature for an off-line synthesis problem.

(6) The algorithm outlined can be conveniently programed as an iterative, interactive multivariable synthesis procedure.

Example 2 given in the section entitled "Numerical Examples" is now used to highlight the features of the spectral synthesis algorithm. Applying the algorithm step by step to the problem of example 2 yields the following synthesis sequence:

(1) First mode $(k = 1)$:

$$\lambda_1 = -1$$

$$z_1^T = (1 \quad 0)$$

$$\Delta^{(1)} = \{1,2,3\}$$

Choose $r = 1$. Then

$$C_1 = (1 \quad 1)$$

$$g_1^{(1)} = (1 \quad 0)^T$$

$$\sigma_1 = 1$$

Since $\sigma_1 \neq 0$, the first eigenvector can be synthesized as $v_1 = (1 \quad 0 \quad 1)^T$; and the transformation matrix $Q^{(1)}$ becomes

$$Q^{(1)} = \begin{bmatrix} 1 & 0 & 0 \\ 0 & 1 & 0 \\ -1 & 0 & 1 \end{bmatrix}$$

(2) Second mode (k = 2):

$$\lambda_2 = -2$$

$$z_2^T = (-1 \quad 1)$$

$$\Delta^{(2)} = \{2,3\}$$

Choose r = 2. Then

$$C_2 = (0.5 \quad 0.5)$$

$$g_2^{(2)} = (0 \quad 1)^T$$

$$\sigma_2 = 1$$

Since $\sigma_2 \neq 0$, the second eigenvector can be synthesized as $v_2 = (-1 \quad 1 \quad 0)^T$; and the transformation $Q^{(2)}$ becomes

$$Q^{(2)} = \begin{bmatrix} 1 & 1 & 0 \\ 0 & 1 & 0 \\ -1 & 1 & 1 \end{bmatrix}$$

(3) Third mode (k = 3):

$$\lambda_3 = -1$$

$$z_3^T = (-1 \quad 1)$$

$$\Delta(3) = \{3\}$$

Thus $r = 3$. Then

$$C_3 = (1 \quad 1)$$

$$g_3^{(3)} = \begin{bmatrix} 0 & 0 \end{bmatrix}^T$$

$$\sigma_3 = 0$$

Since $\sigma_3 = 0$, the third eigenvector cannot be synthesized. Further, since $g_3^{(3)} = \begin{bmatrix} 0 & 0 \end{bmatrix}^T$, the eigenvalue specification cannot be met. This result is obvious since the "basis" vectors spanning the two-dimensional subspace corresponding to $\lambda_1 = -1$ are

$$\begin{bmatrix} 1 & 0 \\ 0 & 1 \\ 1 & 1 \end{bmatrix}$$

and $\{v_1, v_2\}$ already span this subspace. Thus, a second eigenvector associated with $\lambda = -1$ cannot be synthesized as revealed by the null vector $g_3^{(3)}$. This result implies λ_3 must be perturbed slightly. Let $\lambda_3 = (-1 - \epsilon)$; $\epsilon > 0$. Then

$$C_3 = \left(\frac{1}{1+\epsilon} \quad \frac{1}{1+\epsilon} \right)$$

$$g_3^{(3)} = \left(\frac{-\epsilon}{1+\epsilon} \quad \frac{-\epsilon}{1+\epsilon} \right)^T$$

and again $\sigma_3 = 0$; thus, the third eigenvector still cannot be synthesized. In this case, since $g_3^{(3)}$ is not the null vector, the eigenvalue specification can be met but the eigenvector specification requires slight perturbation. Let $z_3^T = (-1 \quad 1 + \delta)$; $\delta \neq 0$. Then

$$\sigma_3 = \frac{-\epsilon\delta}{1+\epsilon} \neq 0$$

and v_3 can now be synthesized as

$$v_3 = \left(-1 \quad 1+\delta \quad \frac{\delta}{1+\epsilon}\right)^T$$

The closed-loop modal matrix V is

$$V = \begin{bmatrix} 1 & -1 & -1 \\ 0 & 1 & 1+\delta \\ 1 & 0 & \frac{\delta}{1+\epsilon} \end{bmatrix}$$

and $\Lambda = \text{Diag}\,[-1 \quad -2 \quad -1-\epsilon]$. Further

$$\left|\det\,[V]\right| = \sigma_3 = \frac{\delta\epsilon}{1+\epsilon}$$

since $\sigma_1 = \sigma_2 = 1$. Thus, in this case, setting a tolerance on the value of σ_3 would directly control the numerical ill-conditioning of V and consequently influence the choice of the perturbations ϵ and δ.

It is also interesting to note that if the sequence of assignment of modes were changed to $\lambda_1 = -1$, $\lambda_2 = -1$, and $\lambda_3 = -2$, then both eigenvectors corresponding to $\lambda_1 = -1$ could be synthesized as

$$[v_1 : v_2] = \begin{bmatrix} 1 & -1 \\ 0 & 1 \\ 1 & 0 \end{bmatrix}$$

and $\lambda_3 = -2$ could still be assigned without perturbation since $g_3^{(3)} = (-0.5 \quad -0.5)^T$. However, the eigenvector specification could not be met since $\sigma_3 = 0$. Thus, a perturbation in z_3^T would allow completion of the synthesis.

MODAL SENSITIVITY ANALYSIS

One of the primary objectives of a feedback control design is to insure that system responses remain well behaved under variations in plant parameters. It is possible to derive quantitative robustness measures for eigenvalue and eigenvector perturbations due to plant variations using the following sensitivity analysis detailed in reference 7.

The closed-loop system satisfies

$$\hat{A}v_i = \lambda_i v_i \qquad (i = 1,2,\ldots,n) \tag{19}$$

Then for first-order differential changes in equation (19),

$$d\hat{A}\, v_i + \hat{A}\, dv_i = \lambda_i\, dv_i + d\lambda_i\, v_i \tag{20}$$

For real eigenvalues let t_i be a dual vector so that

$$\hat{A}^T t_i = \lambda_i t_i \tag{21}$$

By premultiplying equation (20) by t_i^T and using equation (21) the real eigenvalue perturbation can be expressed as

$$d\lambda_i = \frac{t_i^T\, d\hat{A}\, v_i}{t_i^T v_i} \tag{22}$$

The corresponding eigenvector change is given by

$$dv_i = \sum_{j=1}^{n-1} d_{ij} v_i \tag{23}$$

with

$$d_{ij} = \begin{cases} 0 & (i = j) \\ \dfrac{t_j^T (d\hat{A}) v_i}{(\lambda_i - \lambda_j)(t_j^T v_j)} & (i \neq j) \end{cases}$$

Similar expressions can be easily developed for complex conjugate pairs. (See ref. 6.) From equations (22) and (23), bounds can be established for the eigenvalue/eigenvector changes as

$$|d\lambda_i| \leq \frac{\|d\hat{A}\| \, \|v_i\| \, \|t_i\|}{|t_i^T v_i|} = \pi_i \|d\hat{A}\| \tag{24}$$

where

$$\pi_i = \frac{\|v_i\| \, \|t_i\|}{|t_i^T v_i|} \tag{25}$$

where π_i is defined as the "mode condition number" corresponding to the eigenvalue λ_i and clearly $\pi_i \geq 1$. If the eigenvectors v_i are normalized so that

$$v_i^T v_i = t_i^T v_i = 1 \tag{26}$$

Then $\pi_i = \|t_i\|_2$ and

$$|d\lambda_i| \leq \pi_i \|d\hat{A}\|_2 \tag{27}$$

where $\|t_i\|_2 = t_i^T t_i$ and $\|d\hat{A}\|_2 = \sqrt{\text{Maximum eigenvalue of } \left[d\hat{A}^T \cdot d\hat{A}\right]}$.

Similarly, the corresponding bound for eigenvector perturbation is given by

$$\|dv_i\|_2 \leq \|d\hat{A}\|_2 \sum_{\substack{j=1 \\ j \neq i}}^{n} \frac{\pi_j}{|\lambda_i - \lambda_j|}$$

The condition numbers π_i in equation (27) provide quantitative robustness measures for the nominal eigenvalues and eigenvectors of the closed-loop system $\hat{A}$. It is also clear that for plant perturbations not known a priori, the system has best robustness properties if $\pi_i = 1$ $(i = 1,2,\ldots,n)$, which implies that the nominal modal matrix V is orthonormal with $t_i = v_i$ $(i = 1,2,\ldots,n)$.

From equation (8) it is apparent that sufficient eigenvector freedom is generally unavailable to construct an orthonormal modal matrix. Thus, from a practical design perspective it is better to seek a mode-decoupled design, with each state variable dominantly displaying one mode (as determined by a dominant eigenvector entry). This design, in the limit when total decoupling is possible, results in an orthonormal V. Further, if the perturbations dA are known a priori, then the appropriate zero sensitivity eigenvectors span the null space of dA, and if such an eigenvector can be synthesized by using state feedback, the corresponding eigenvalue will be invariant to the specified dA.

The mode condition numbers π_i derived as the norm of the dual vectors t_i (eq. (27)) also directly relate to the numerical ill-conditioning of the modal matrix V for inversion (linear dependence of eigenvectors). This fact becomes apparent by considering the relation

$$\begin{bmatrix} t_1^T \\ \cdots \\ t_2^T \\ \cdots \\ \vdots \\ t_n^T \end{bmatrix} \left[v_1 : v_2 : \cdots : v_n \right] = I_n \qquad (28)$$

and noting that as the eigenvectors v_i tend toward being linearly dependent, the norms of the corresponding dual vectors t_i increase in order to satisfy the constraint equation (28). Thus, large values of π_i indicate that the system has poor robustness properties and also reinforce the fact that the corresponding modal matrix is ill-conditioned. It should be recalled that the spectral synthesis algorithm described earlier allows the designer to efficiently control this system robustness property by setting a numerical tolerance on the σ_k of equation (18) to pass the test $\sigma_k \neq 0$ in steps 4 and 5 of the algorithm. Since the determinant of V is obtained as the product of the σ_k $(k = 1,2,\ldots,n)$, it is clear that the design process effectively controls the ill-conditioning of V for inversion.

AIRCRAFT LATERAL CONTROL SYSTEM SYNTHESIS

In this section, the lateral performance objectives of an aircraft are formulated as an eigenvalue/eigenvector assignment problem and the utility of the spectral synthesis algorithm is demonstrated by designing a feedback control system for a fighter aircraft. Major qualitative design objectives for lateral aircraft dynamics are

(a) Fast roll rate response with minimum overshoot

(b) Good Dutch roll damping

(c) Low sideslip and peak lateral acceleration in response to roll stick command, for good turn coordination

(d) Low roll response to sideslip gust inputs.

Performance Specification

The quantitative performance specifications can be briefly summarized as follows (ref. 8):

(1) The frequency and damping of the Dutch roll mode shall satisfy

$$\zeta_d > 0.19$$

$$\omega_{nd} > 1.0$$

$$\zeta_d \omega_{nd} > 0.35$$

(2) If the spiral mode is unstable, the time to double shall be greater than 20 seconds.

(3) The roll-subsidence time constant τ_R shall be less than 1.0 second.

(4) After a rudder-pedals-free step aileron command, the ratio of sideslip to the parameter θ shall be less than that specified below. The aileron command shall be held fixed until the bank angle has changed at least 90^o.

(a) Category A (rapid maneuvering phase)

$\beta/\theta < 6^o$ for adverse sideslip

$\beta/\theta < 2^o$ for proverse sideslip

(b) Category C (take off/landing phase)

$\beta/\theta < 10^{o}$ for adverse sideslip

$\beta/\theta < 3^{o}$ for proverse sideslip

The parameter θ is given by

$$\theta = \frac{\phi_t}{90^{o}} \qquad (t = 1.3)$$

for category A and

$$\theta = \frac{\phi_t}{30^{o}} \qquad (t = 1.0)$$

for category C, where ϕ_t is the bank angle achieved at t seconds after the step input.

(5) For a step aileron command held until the bank angle has changed at least 90^{o}, the roll rate at the first minimum following the first peak shall be at least 60 percent of the peak value.

(6) For category A turn coordination, the lateral acceleration at the pilot shall be less than 0.15g for a 60^{o}/sec roll to a 60^{o} bank.

It should be recognized that these aircraft response characteristics must usually be achieved under feedback gain magnitude constraints arising because of sensor noise and other considerations. For the numerical aircraft example to be discussed in the section entitled "Fighter Aircraft Control Analysis," all the feedback gain magnitudes were constrained to be about unity. The aircraft performance in the numerical example is evaluated by using the linearized model at selected flight conditions.

Aircraft Model and Design Considerations

The nonlinear equations of motion of the aircraft are used to generate linear perturbation models at various flight conditions. Accordingly, the state space representation, referenced to the stability axes, takes the form

$$\left.\begin{aligned} \dot{x} &= Ax + Bu \\ y &= Cx + Du \end{aligned}\right\} \qquad (29)$$

where

$$A = \begin{bmatrix} L'_p & L'_r & L'_\beta & 0 \\ N'_p & N'_r & N'_\beta & 0 \\ Y_p & Y_r & Y_\beta & g/V_0 \\ 1 & 0 & 0 & 0 \end{bmatrix} \qquad B = \begin{bmatrix} L'_{\delta_a} & L'_{\delta_r} \\ N'_{\delta_a} & N'_{\delta_r} \\ Y_{\delta_a} & Y_{\delta_r} \\ 0 & 0 \end{bmatrix}$$

$$C = \begin{bmatrix} 1 & 0 & 0 & 0 \\ 0 & 0 & 0 & 0 \\ M_p & M_r & M_\beta & M_\phi \\ 0 & 0 & 0 & 1 \end{bmatrix} \qquad D = \begin{bmatrix} 0 & 0 \\ 0 & 0 \\ M_{\delta_a} & M_{\delta_r} \\ 0 & 0 \end{bmatrix}$$

with $x^T = (p\ \dot{\psi}\ \beta\ \phi)$; $u^T = (\delta_a : \delta_r)$; $y^T = (p\ \dot{\psi}\ a_y\ \phi)$.

For the aircraft control problem, from sensor considerations, feedback from β variable is difficult to implement. Hence, the control laws are derived by using the output vector y of equation (29), where the lateral acceleration a_y sensor substitutes for the sideslip β sensor. The state feedback law of equation (2) is modified as finding a control law of the form

$$u = \tilde{K}y + u_p \tag{30}$$

such that the closed-loop system meets desired eigenvalue/eigenvector specifications, with $\tilde{K}$ the output feedback matrix and u_p the external pilot input. The closed-loop system after applying feedback law (30) takes the form

$$\left.\begin{aligned} \dot{x} &= \left[A + B\hat{K}C\right]x + BP\,u_p \\ y &= \left[C + D\hat{K}C\right]x + DP\,u_p \end{aligned}\right\} \tag{31}$$

where $P = \left[I_m - \tilde{K}D\right]^{-1}$ and $\hat{K} = P\tilde{K}$ is the equivalent output feedback matrix obtained by setting $D = 0$. $\tilde{K}$ exists provided P exists. Further, the feedback law (30) is still equivalent to the state feedback case since C is rank n for all flight conditions. Thus, for every state feedback law $u = Kx + u_p$ (eq. (2)) derived by using the spectral synthesis algorithm, there exists an equivalent output feedback matrix $\tilde{K}$ (eq. (30) given by

$$\tilde{K} = K\left[C + DK\right]^{-1} \tag{32}$$

Direct matrix manipulations show that the inverse of the matrix $\left[C + DK\right]$ in equation (32) exists if P exists. Hence, the theory developed for the state variable feedback problem is directly applicable to the aircraft lateral dynamics model described by equation (29).

Appendix B gives the numerical values for the (A,B,C,D) quadruple of equation (29) for a typical fighter aircraft at selected flight conditions. An examination of these models over the complete flight envelope reveals that the following system constraints contribute critically to the evolution of a satisfactory closed-loop system.

The large L'_β derived in most of the flight conditions indicates that significant roll motions are induced for sideslip gust inputs. A feedback augmentation to reduce this effect yields the following control equations:

$$\hat{L}'_\beta = L'_\beta + L'_{\delta_a} k_{A_\beta} + L'_{\delta_r} k_{R_\beta}$$

with

$$\left[k_{A_\beta} \vdots k_{R_\beta}\right]^T = \frac{1}{\hat{M}_\beta}\left[k_{A_{a_y}} \vdots k_{R_{a_y}}\right]^T$$

and

$$\hat{M}_\beta = M_\beta + M_{\delta_a} k_{A_\beta} + M_{\delta_r} k_{R_\beta}$$

with the circumflex ($\hat{}$) denoting closed-loop magnitudes.

It should be noted that if the gain magnitudes $k_{A_{a_y}}$ and $k_{R_{a_y}}$ are constrained, substantial reduction in the $\hat{L}'_\beta$ magnitude are possible only if the magnitude of the control derivatives L'_{δ_a}, L'_{δ_r}, and M_β are large. Further, since the M_β magnitude is dependent on the a_y sensor location, a possibility exists to optimally locate the acceleration sensor from a control viewpoint.

For satisfactory turn coordination, β and a_y excitation at the pilot station must be minimized for aileron input. This minimization implies reduction of cross coupling between the roll dynamics and the sideslip/yaw rate. This coupling arises not only because of mode cross coupling in the system matrix A, but also because of the input mixing through the control matrix B.

Whereas feedback is effective only in suppressing the intervariable cross coupling in A, some form of precompensation is necessary to minimize the input mixing of B. Thus, L'_r, L'_β, N'_p, and Y_p must be reduced by feedback. Again, the feedback magnitude constraints determine the limit of reduction. Thus, if the turn coordination specification cannot be met by feedback alone, a feedforward compensation, in the form of an aileron/rudder interconnect, must be introduced to increase the ratio $L'_{\delta_a}/Y'_{\delta_a}$. The resulting composite control law takes the form

$$u = \tilde{K}y + Hu_p \tag{33}$$

where $u_p = (\delta_A : \delta_R)^T$ is the external pilot input and H is a 2×2 nonsingular feedforward matrix representing aileron/rudder interconnect. The closed-loop system after applying feedback law (33) takes the form

$$\left.\begin{aligned} \dot{x} &= \left[A + B\hat{K}C\right]x + BPH\,u_p \\ y &= \left[C + D\hat{K}C\right]x + DPH\,u_p \end{aligned}\right\} \tag{34}$$

where $\hat{K}$ and P are defined in equation (31).

Eigenvalue/Eigenvector Assignment Formulation

The aircraft handling characteristics postulated earlier can be summarized as lateral dynamics being composed of two weakly coupled subsystems. Roll rate and bank angle constitute the first subsystem and display predominantly the roll subsidence and spiral modes. The second subsystem is characterized by a well damped Dutch roll mode defining the yaw rate and sideslip motions. This results in the mode (eigenvalue) and associated response variable (eigenvector shape) assignments of table I.

TABLE I.- DESIRED MODAL SPECIFICATIONS

Mode	Dominant response variable
Roll subsidence	Roll rate, p
Spiral	Bank angle, ϕ
Dutch roll	Yaw rate and sideslip, $\dot{\psi}, \beta$

TABLE II.- DESIRABLE CLOSED-LOOP MODAL STRUCTURE

Eigenvector components	Roll subsidence mode	Dutch roll mode		Spiral mode
p	1	0	z_{13}	z_{14}
$\dot{\psi}$	0	1	1	z_{24}
β	w_{11}	w_{12}	w_{13}	w_{14}
ϕ	w_{12}	w_{22}	w_{23}	w_{24}

It should be emphasized that the structure in table II is only one of several configurations that can be selected. In practice, alternative structures must be tried to effectively trade off different (often conflicting) performance specifications.

In this report, the rationale for the selection of the z_{ij} components in table II was to meet the mode decoupled structure postulated in table I. This structure, in addition to meeting the handling quality specification, would result in robust feedback designs.

The roll subsidence mode design vector selection is straightforward. The Dutch roll mode eigenvector design parameters were selected to keep only one parameter (z_{13}) available for manipulation in the design iteration cycles. The parameter z_{13} directly influences the closed-loop L'_β magnitude and is selected to effect the desired reduction in L'_β magnitude. The spiral mode eigenvector components z_{14} and z_{24} must be selected so that the bank angle response is dominated by the spiral mode.

The β and ϕ components (w_{ij} elements) of the eigenvectors in table II are computed by using constraint equation (8) or (A5), after specifying the appropriate eigenvalues. The eigenvalues must be selected to meet quantitative speed of response and at the same time yield desirable eigenvector forms. The mode coupling matrices C_i (eq. (10)) clearly define this constraint relationship, and aid in the selection of the appropriate eigenvalues.

It is helpful at this stage to clarify these design concepts by using a numerical example. Consider the aircraft model corresponding to flight condition 1 (appendix B). In particular, consider the synthesis of the spiral mode eigenvector. The spiral mode eigenvalue can lie in the range -0.01 to -0.1. The design equations take the form (eq. (10)). For $\lambda = -0.01$,

$$\begin{bmatrix} w_{14} \\ w_{24} \end{bmatrix} = \begin{bmatrix} -25.52 & -7.16 \\ -100 & -6.02 \end{bmatrix} \begin{bmatrix} z_{14} \\ z_{24} \end{bmatrix} \tag{35}$$

Judicious choice of z_{14} and z_{24} can now be made by examining the modal coupling relations in equation (35) to meet the requirement that w_{24} be very large compared with w_{14}, z_{14}, and z_{24}. One acceptable solution is obtained by selecting $z_{24} = -3.5z_{14}$; as a result, the normalized eigenvector (with $v_4^T v_4 = 1$) is obtained as

$$v_4^T = (z_{14}\ z_{24}\ w_{14}\ w_{24}) = (-0.012\ 0.044\ 0.006\ 0.998) \tag{36}$$

which has the desired bank angle dominant structure. Suppose, on the other hand, that if the spiral mode is chosen as $\lambda = 0.1$, the design equations become

$$\begin{bmatrix} w_{14} \\ w_{24} \end{bmatrix} = \begin{bmatrix} -4.52 & -11.59 \\ -10 & -0.6 \end{bmatrix} \begin{bmatrix} z_{14} \\ z_{24} \end{bmatrix} \tag{37}$$

and thus the eigenvector structure would be worse compared with that in equation (36). Thus, a trade-off between speed of response and minimal influence of the slow spiral mode on the response of $\dot{\psi}$ and β would finally determine the spiral mode in the range -0.01 to -0.1. This analysis also highlights the fact that mode selection is not only dictated by speed of response but also by the eigenvector structure it generates through the mode coupling matrices C_i (eq. (10)). In the design of the spiral mode eigenvector, it sould be emphasized that suppression of this slow mode from the β response is vital in limiting steady-state β excursions under the roll-stick command.

The synthesis procedure up to this stage can be summarized as consisting of the following steps:

Step 1.- For each mode i compute the eigenvector coupling matrix C_i (eq. (10)) for the range of assignable values.

Step 2.- Select the mode from step 1 which yields the eigenvector structure closest to the desired one by appropriately choosing the z vectors as illustrated in the numerical example.

Step 3.- Complete the synthesis by specifying all the modes and design vectors and applying the spectral synthesis algorithm.

It is very likely that a design in step 3 may violate gain magnitude constraints. The design parameters must then be iteratively modified to meet

these constraints. The direction of parameter change is found by studying the open loop modal structure and identifying the design specifications that unduly violate the physics of the basic plant. For example, the z_{13} parameter directly determines the reduction of the L'_{β} derivative and consequently controls the magnitude of the feedback gains $k_{A_{a_y}}$ and $k_{R_{a_y}}$.

FIGHTER AIRCRAFT CONTROL ANALYSIS

Twenty flight conditions describing the operational flight envelope of the aircraft are shown in figure 1. The design points are represented as a plot of Mach number against angle of attack. The altitude parameter is identified with different symbols. Linearized state variable models describing the lateral dynamics at each of these flight conditions were used for the synthesis analysis. The flight conditions of figure 1 were classified into three catagories as shown in table III. The group numbers are arranged in decreasing order of control effectiveness as measured by the magnitudes of the control derivatives L'_{δ_a} and L'_{δ_r}, with group III flight conditions posing the worst conditions for synthesis from a mode decoupling viewpoint.

TABLE III.- FLIGHT CONDITION CLASSIFICATION

Flight group	Flight conditions*
I	1, 2, 3, 4, 6, 9, 10, 12, 13, 14, 19, 20
II	5, 7, 8, 11, 15, 16
III	17, 18

*See figure 1.

Feedback Design

The basic modal matrix structure of table II was employed for the flight conditions in groups I and II. The design parameter z_{13} ranged from -0.2 to -1 for group I and -2 to -4 for group II to meet the gain constraint requirements on the lateral acceleration sensor. Larger magnitudes of z_{13} implied increased roll response to β gust inputs. As mentioned earlier, significant changes in the basic aircraft characteristics could not be achieved for low altitude and low Mach number flight conditions, namely, flight conditions 17 and 18. Low control derivative magnitudes coupled with feedback gain limitations contributed to the problem. For these cases, the iterative design process was initiated with the Dutch roll mode eigenvector structure corresponding to that of the free aircraft. Final trimming of the design parameters and Dutch roll mode damping were effected to give a reasonable improvement in response with acceptable feedback gains.

Precompensation Design

As noted earlier, if the turn coordination specification cannot be achieved by mode decoupling alone (through feedback), additional feedforward compensation by the aileron/rudder interconnect is required. In order to meet the roll stick input specification, the following structure for the precompensation matrix H (eq. (33)) was found to be satisfactory

$$H = \begin{bmatrix} 1 & 0 \\ k_{R_A} & 1 \end{bmatrix} \tag{38}$$

The interconnect gain k_{R_A} is determined to maximize the ratio of $\hat{L}'_{\delta_a} / \hat{Y}_{\delta_a}$.

CONTROL AUGMENTED AIRCRAFT PERFORMANCE

The modal control procedure was used to obtain the gain matrices $\tilde{K}$ and H (eq. (33)) at all 20 design flight conditions summarized in figure 1. The next objective is to evolve a control system which operates over the flight envelope based on these fixed point designs. This procedure usually takes the form of developing gain schedules using appropriate air data parameters as scheduling parameters. However, in this report the question of gain scheduling will not be pursued; instead, the improvement in system performance, based on fixed point designs is shown at three selected design flight conditions 1, 17, and 20. These flight conditions cover comprehensively the complete flight envelope from the synthesis complexity viewpoint. Flight condition 1 represents the nominal cruise condition with no significant synthesis constraints. Flight condition 20 is a high-angle-of-attack condition usually known to result in poor lateral control and turn coordination (ref. 8). Finally, flight condition 17 covers the landing approach condition and represents the most difficult flight regime from a mode decoupling viewpoint.

Tables IV to VI detail the eigenvalue/eigenvector modifications achieved at these flight conditions. In tables IV to VII, $j = \sqrt{-1}$. The results are based on the control law given in the respective tables. It is worthwhile noting the modification achieved in the eigenvector pair corresponding to the Dutch roll mode in flight conditions 1 and 20. The desired decoupling of the roll rate variable from the Dutch roll mode could be achieved only by assigning an overdamped complex pair of eigenvalues ($-1.5 \pm j0.75$) as the Dutch roll mode. Further, the design iterations revealed that the Dutch roll mode damping could not be reduced (to improve $\dot{\psi}$ and β responses) without violating feedback gain limits on the a_y sensor.

TABLE IV.- MODAL CHARACTERISTICS (FLIGHT CONDITION 1)

$[j = \sqrt{-1}]$

Eigenvector components	Characteristic for free aircraft eigenvalue of -				Characteristic for augmented aircraft eigenvalue of -			
	-3.70	-0.03	-0.34 ± j2.66		-6.00	-0.01	-1.5 ± j0.75	
p	-0.964	-0.032	-0.403	0.829	0.986	0.013	0.	-0.117
ψ	-0.041	0.044	-0.096	-0.131	0.	-0.045	0.586	0.586
β	0.002	0.002	0.069	-0.034	-0.008	-0.0004	0.137	0.527
ϕ	0.261	0.998	0.314	0.112	-0.164	-0.999	-0.041	0.034

CONTROL LAW (eq. (33))

$$\tilde{K} = \begin{bmatrix} -0.204 & -0.491 & -0.799 & 0.017 \\ -0.152 & 0.318 & -0.504 & -0.021 \end{bmatrix}$$

$$H = \begin{bmatrix} 1 & 0 \\ 0.325 & 1 \end{bmatrix}$$

TABLE V.- MODAL CHARACTERISTICS (FLIGHT CONDITION 17)

$[j = \sqrt{-1}]$

Eigenvector components	Characteristic for free aircraft eigenvalue of -				Characteristic for augmented aircraft eigenvalue of -			
	-1.97	-0.063	-0.168 ± j1.594		-4.5	-0.07	-0.5 ± j0.9	
p	-0.89	-0.078	-0.63	0.556	0.976	-0.086	-0.49	0.49
ψ	-0.039	0.139	-0.03	-0.075	0.	0.140	-0.074	-0.098
β	-0.001	0.017	0.122	-0.005	-0.017	-0.004	0.139	-0.173
ϕ	0.454	0.987	0.381	0.357	-0.217	0.986	0.643	0.198

CONTROL LAW (eq. (33))

$$\tilde{K} = \begin{bmatrix} -1.07 & 0.595 & -1.259 & -0.294 \\ -0.179 & 0.362 & -0.171 & -0.084 \end{bmatrix}$$

$$H = \begin{bmatrix} 1 & 0 \\ -0.069 & 1 \end{bmatrix}$$

TABLE VI.- MODAL CHARACTERISTICS (FLIGHT CONDITION 20)

$[j = \sqrt{-1}]$

Eigenvector components	Characteristic for free aircraft eigenvalue of -				Characteristic for augmented aircraft eigenvalue of -			
	-0.77	-0.096	-1.034 ± j2.898		-6.0	-0.01	-1.5 ± j0.75	
p	0.588	0.102	-0.046	0.946	0.986	-0.022	0.	-0.116
$\dot{\psi}$	0.11	-0.022	-0.022	0.005	0.	0.045	0.578	0.578
β	-0.022	-0.007	0.077	-0.028	-0.044	0.0004	0.113	0.544
ϕ	-0.801	-0.995	0.296	-0.087	-0.164	0.999	-0.073	-0.066

CONTROL LAW (eq. (33))

$$\bar{K} = \begin{bmatrix} -0.357 & -0.305 & -0.847 & -0.001 \\ -0.083 & 0.581 & 0.051 & -0.033 \end{bmatrix}$$

$$H = \begin{bmatrix} 1 & 0 \\ -0.02 & 1 \end{bmatrix}$$

Table VII depicts the improvement in the aircraft robustness characteristics in terms of the mode condition numbers introduced in the section entitled "Modal Sensitivity Analysis." Significant improvement in system sensitivity characteristics has been achieved in flight conditions 1 and 20. However, the improvement in sensitivity performance in flight condition 17 is marginal and is due to the inability to appreciably decouple Dutch roll mode from p and ϕ variables. In table VII the determinant of the modal matrix V with eigenvectors normalized as $v_i^T v_i = 1$ is also included. It is evident from table VII that the determinant of V reflects the aggregate effect of all the mode condition numbers (π_i). The determinant value decreases as the mode condition numbers increase.

Finally, time response histories for roll stick input and sideslip gust inputs are compared in figures 2 and 3. From the response curves it is apparent that control augmentation has reduced the cross coupling between the roll axis (p,ϕ) and the yaw axis ($\dot{\psi}$,β). It is also important to note that in figures 2(a) and 2(c), feedback augmentation has reduced the peak roll rate capability for pilot aileron input. This reduction can be offset by introducing appropriate gain factors in the forward loop (H matrix (eq. (33))). It should be noted that the roll response to sideslip gust input has been significantly reduced in figures 3(a) and 3(c). Finally, for flight condition 20 the quantitative β/θ performance specification could not be met but was significantly improved compared with the free aircraft performance. In all other flight conditions the feedback system met all the lateral handling criteria postulated earlier.

TABLE VII.- AIRCRAFT MODAL SENSITIVITY CHARACTERISTICS

Flight condition	Free aircraft		Augmented aircraft	
	Eigenvalue	Mode condition number, π_i	Eigenvalue	Mode condition number, π_i
1	-3.70 -0.03 -0.34 ± j2.66	10.39 2.27 14.09	-6.0 -0.01 -1.5 ± j0.75	1.065 1.027 4.337
17	-1.97 -0.06 -0.17 ± j1.59	6.76 3.52 9.68	-4.5 -0.07 -0.5 ± j0.9	3.51 3.17 6.817
20	-0.77 -0.096 -1.03 ± j2.9	8.62 6.36 14.32	-6.0 -0.01 -1.5 ± j0.75	1.069 1.021 4.0

Flight condition	Free aircraft Det [V]	Augmented aircraft Det [V]
1	-0.0146	-0.225
17	-0.0202	0.0412
20	-0.0086	0.242

CONCLUDING REMARKS

A new multivariable synthesis procedure for aircraft handling qualities design has been developed. The synthesis procedure is computationally simple in that it only involves solution of linear systems of equations. This results in an efficient computer-aided interactive design tool for flight control system synthesis. It is shown that the quantitative lateral design objectives can be conveniently formulated as an eigenvalue/eigenvector assignment problem. By noting the freedom available in the selection of eigenvalues and eigenvectors under state variable feedback, a systematic design methodology is evolved to meet the performance specifications. The inherently mode-oriented synthesis procedure provides significant insight into the design process and allows optimizing the response of the aircraft under often conflicting requirements. The study also revealed that the closed-loop modal matrix (matrix of eigenvectors) plays a pivotal role in characterizing system sensitivity to plant parameter variations. New robustness measures related to the numerical ill-conditioning of the modal matrix for inversion, termed mode condition numbers, are also developed.

The synthesis technique is illustrated by using the linearized lateral dynamics model of a typical fighter aircraft. The simulation studies revealed that the feedback-augmented aircraft exhibited improved Dutch roll damping, good turn coordination for pilot roll stick command, and reduced roll response to sideslip gusts over the flight envelope.

Langley Research Center
National Aeronautics and Space Administration
Hampton, VA 23665
April 13, 1978

APPENDIX A

COMPLEX CONJUGATE PAIR IN REAL ARITHMETIC FORM

In order to perform real arithmetic computations with complex conjugate pair eigenvalues, the following transformation is established for reference.

Consider the eigenvalue/eigenvector relation

$$A(q + js) = (a + jb)(q + js) \tag{A1}$$

where $a + jb$ is a complex eigenvalue of A and $q + js$ the associated eigenvector (with $j = \sqrt{-1}$). Equation (A1) can be solved for real and imaginary parts as

$$\left.\begin{aligned} Aq &= aq - bs \\ As &= bq + as \end{aligned}\right\} \tag{A2}$$

with the same relation holding for the conjugate eigenvalue $a - jb$. Equation (A2) can be written as

$$A(q : s) = (q : s)\begin{pmatrix} a & -b \\ b & a \end{pmatrix} \tag{A3}$$

where q and s are real vectors corresponding to the real and imaginary part of the complex eigenvector and the complex conjugate pair of eigenvalues $a \pm jb$ can be written in equivalent real form as

$$\rho = \begin{bmatrix} a & b \\ -b & a \end{bmatrix} \tag{A4}$$

By using the real arithmetic representation for a pair of complex eigenvalues $a_i \pm jb_i$, the eigenvector constraints of equation (8) take the form

APPENDIX A

$$\begin{bmatrix} a_i I_{n-m} - F & \vdots & -b_i I_{n-m} \\ \cdots\cdots & \vdots & \cdots\cdots \\ b_i I_{n-m} & \vdots & a_i I_{n-m} - F \end{bmatrix} \begin{bmatrix} w_i \\ \cdots \\ w_{i+1} \end{bmatrix} = \begin{bmatrix} G + a_i S & \vdots & -b_i S \\ \cdots\cdots & \vdots & \cdots\cdots \\ b_i S & \vdots & G + a_i S \end{bmatrix} \begin{bmatrix} z_i \\ \cdots \\ z_{i+1} \end{bmatrix} \tag{A5}$$

where

$$\left[v_i : v_{i+1}\right] = \begin{bmatrix} z_i & \vdots & z_{i+1} \\ \cdots & \vdots & \cdots \\ w_i & \vdots & w_{i+1} \end{bmatrix}$$

are the real eigenvector pair associated with $a_i \pm jb_i$.

APPENDIX B

AIRCRAFT STATE VARIABLE MODEL AT SELECTED FLIGHT CONDITIONS

The lateral dynamics of the aircraft modeled in state space takes the form

$$\left.\begin{aligned} \dot{x} &= Ax + Bu \\ \bar{y} &= \bar{C}x + \bar{D}u \end{aligned}\right\} \tag{B1}$$

where $x^T = (p \quad \dot{\psi} \quad \beta \quad \phi)$; $u^T = (\delta_a : \delta_r)$; and $\bar{y} = a_y$. For brevity of documentation the state variables p, $\dot{\psi}$, and ϕ are omitted from the output set in equation (B1). The respective quadruples (A, B, $\bar{C}$, $\bar{D}$) for selected flight conditions are listed in tables B1 to B3.

TABLE B1.- FLIGHT CONDITION 1 (NOMINAL CRUISE)

[Mach number, 0.67; altitude, 6096 m (20 000 ft); angle of attack, 3.45°]

A matrix:

-3.79E+00	4.06E-02	-5.20E+01	0.
-1.34E-01	-3.59E-01	4.24E+00	0.
6.02E-02	-9.97E-01	-2.72E-01	4.62E-02
1.00E+00	6.03E-02	0.	0.

B matrix:

2.50E+01	9.83E+00
1.42E+00	-4.20E+00
5.01E-03	5.03E-02
0.	0.

$\bar{C}$ matrix:

-1.25E-01	-6.12E-02	-3.41E+00	-1.50E-03

$\bar{D}$ matrix:

1.03E+00	-2.66E-01

APPENDIX B

TABLE B2.- FLIGHT CONDITION 17 (LANDING APPROACH)

[Mach number, 0.19; altitude, 30 m (98.43 ft); angle of attack, 6.72°]

A matrix:

-1.99E+00	9.21E-01	-1.65E+02	0.
-7.97E-02	-1.77E-01	5.68E-01	0.
1.19E-01	-9.92E-01	-2.01E-01	1.51E-01
1.00E+00	1.18E-01	0.	0.

B matrix:

2.98E+00	1.79E+00
2.47E-02	-7.92E-01
3.50E-03	3.74E-02
0.	0.

$\bar{C}$ matrix:

-6.35E-02	5.93E-03	-9.79E-01	-4.38E-03

$\bar{D}$ matrix:

9.01E-02	-2.89E-02

TABLE B3.- FLIGHT CONDITION 20 (HIGH ANGLE OF ATTACK)

[Mach number, 0.6; altitude, 6096 m (20 000 ft); load factor, g units, 4; angle of attack, 15.44°]

A matrix:

-2.25E+00	7.58E-01	-3.63E+01	0.
-7.03E-02	-4.06E-01	-4.50E-02	0.
2.66E-01	-9.63E-01	-2.83E-01	4.98E-02
1.00E+00	2.76E-01	0.	0.

B matrix:

1.61E+01	8.21E+00
7.25E-01	-3.43E+00
1.90E-04	4.76E-02
0.	0.

$\bar{C}$ matrix:

-1.04E-01	3.13E-01	-3.95E+00	-2.07E-02

$\bar{D}$ matrix:

5.76E-01	-1.93E-01

REFERENCES

1. Harvey, C. A.; Stein, G.; and Doyle, J. C.: Optimal Linear Control (Characterization of Multi-Input Systems). ONR CR 215-238-2, U.S. Navy, Aug. 1977. (Available from DDC as ADA043771.)

2. Porter, Brian; and Crossley, Roger: Modal Control: Theory and Applications. Taylor & Francis (London), 1972.

3. Anderson, B. D. O.; and Luenberger, D. G.: Design of Multivariable Feedback Systems. Instn. Elec. Engrs. - Proc., vol. 114, no. 3, Mar. 1967, pp. 395-399.

4. Chidambara, M. R.; Broen, R. B.; and Zaborszky, J.: A Simple Algorithm for Pole Assignment in a Multiple Input Linear Time Invariant Dynamic System. Trans. ASME, Ser. G: J. Dynamic Systems, Measurement, and Control, vol. 96, no. 1, Mar. 1974, pp. 13-18.

5. Srinathkumar, S.; and Rhoten, R. P.: Eigenvalue/Eigenvector Assignment for Multivariable Systems. Electronic Lett., vol. 11, no. 6, Mar. 1975, pp. 124-125.

6. Srinathkumar, S.: Spectral Characterization of Multi-Input Dynamic Systems. Ph. D Diss., Oklahoma State Univ., 1976.

7. Fadeev, D. K.; and Faddeeva, V. N. (Robert C. Williams, trans.): Computational Methods of Linear Algebra. W. H. Freeman and Co., c.1963.

8. Hartmann, Gary L.; Hauge, James A.; and Hendrick, Russell C.: F-8C Digital CCV Flight Control Laws. NASA CR-2629, 1976.

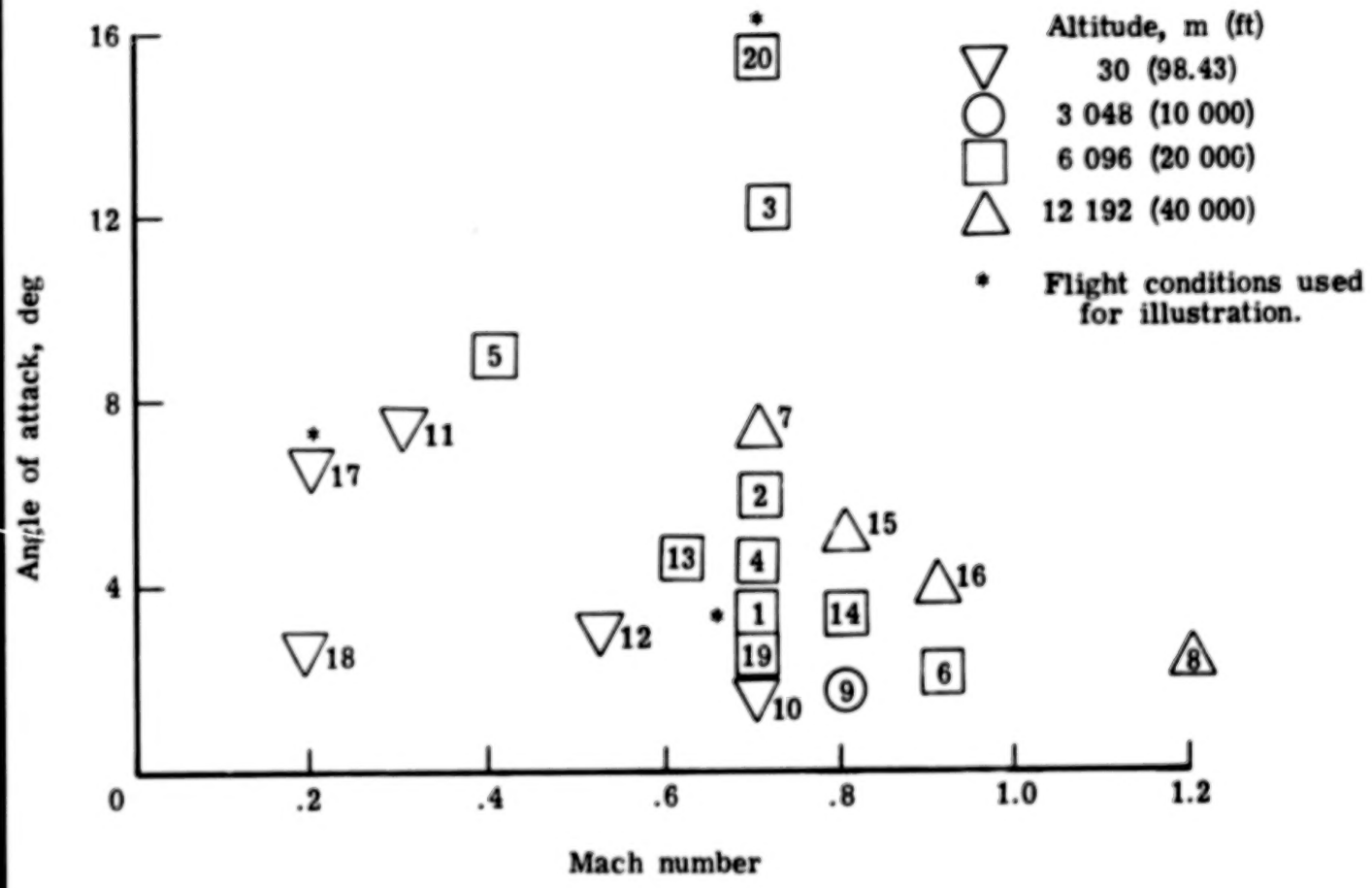

Figure 1.- Aircraft flight envelope and design points.

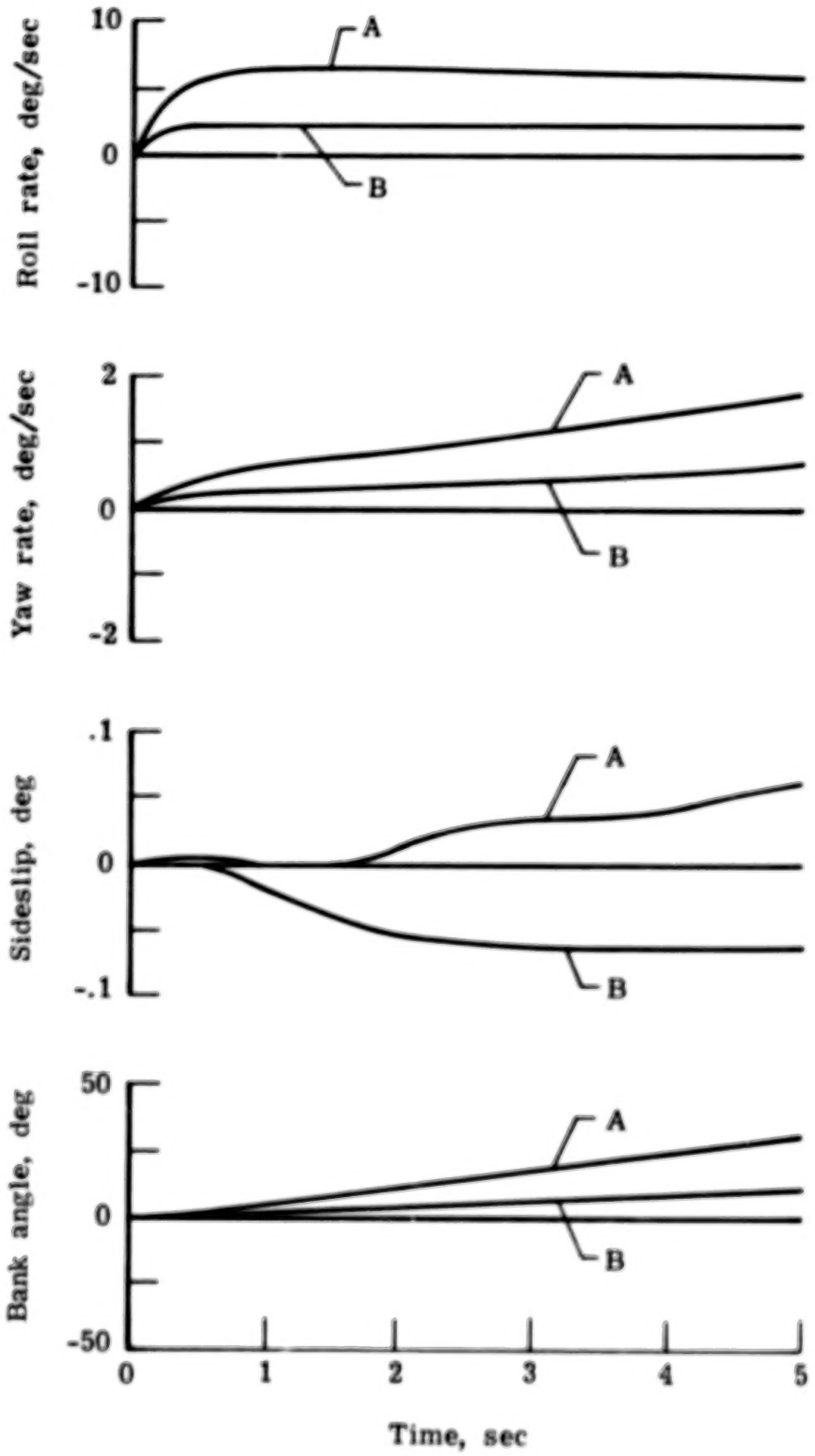

(a) Flight condition 1 (nominal cruise).

Figure 2.- Comparison of free aircraft and augmented aircraft response to roll stick step input. $\delta_A(0) = 1^o$; A indicates free aircraft response and B corresponds to augmented aircraft response.

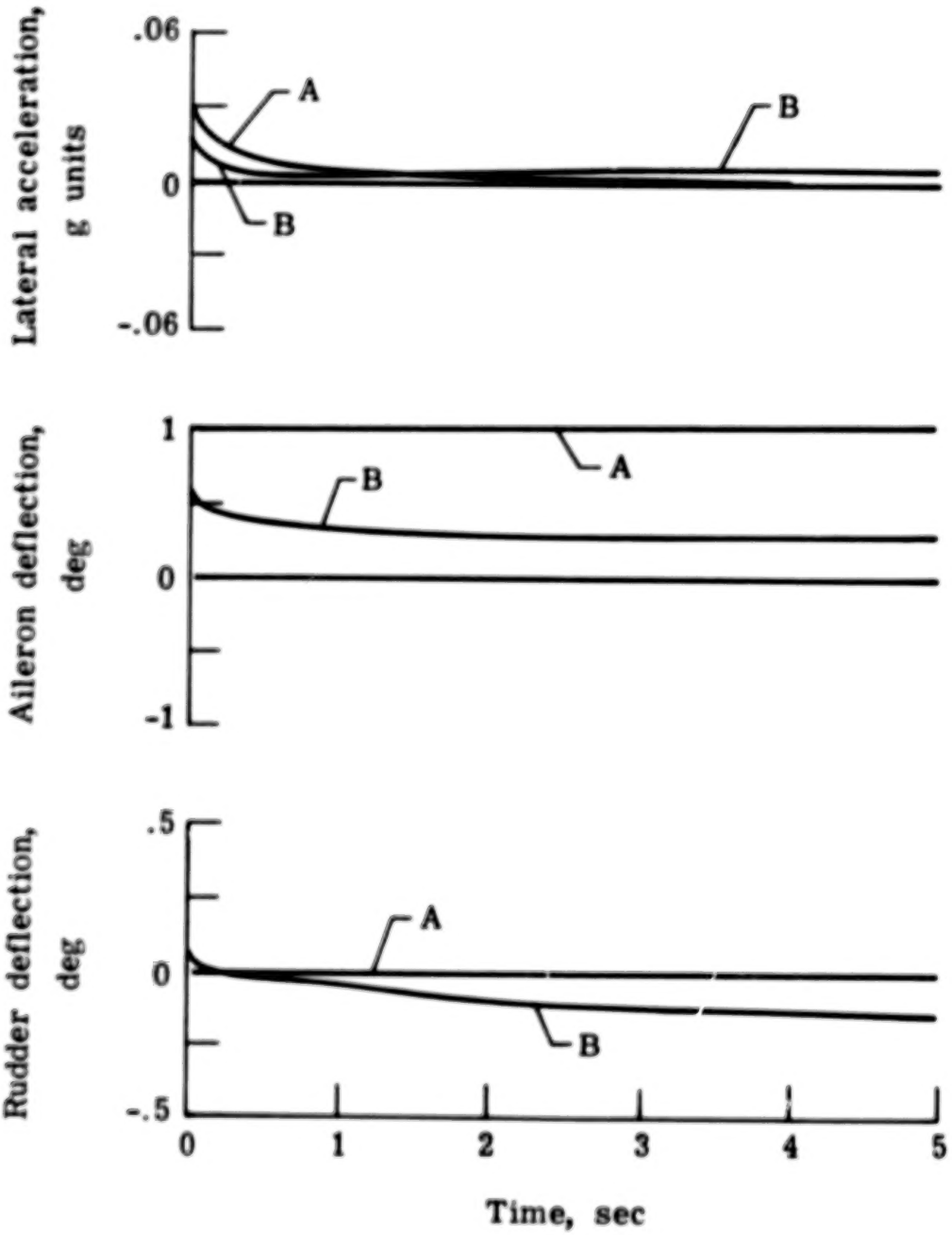

(a) Concluded.

Figure 2.- Continued.

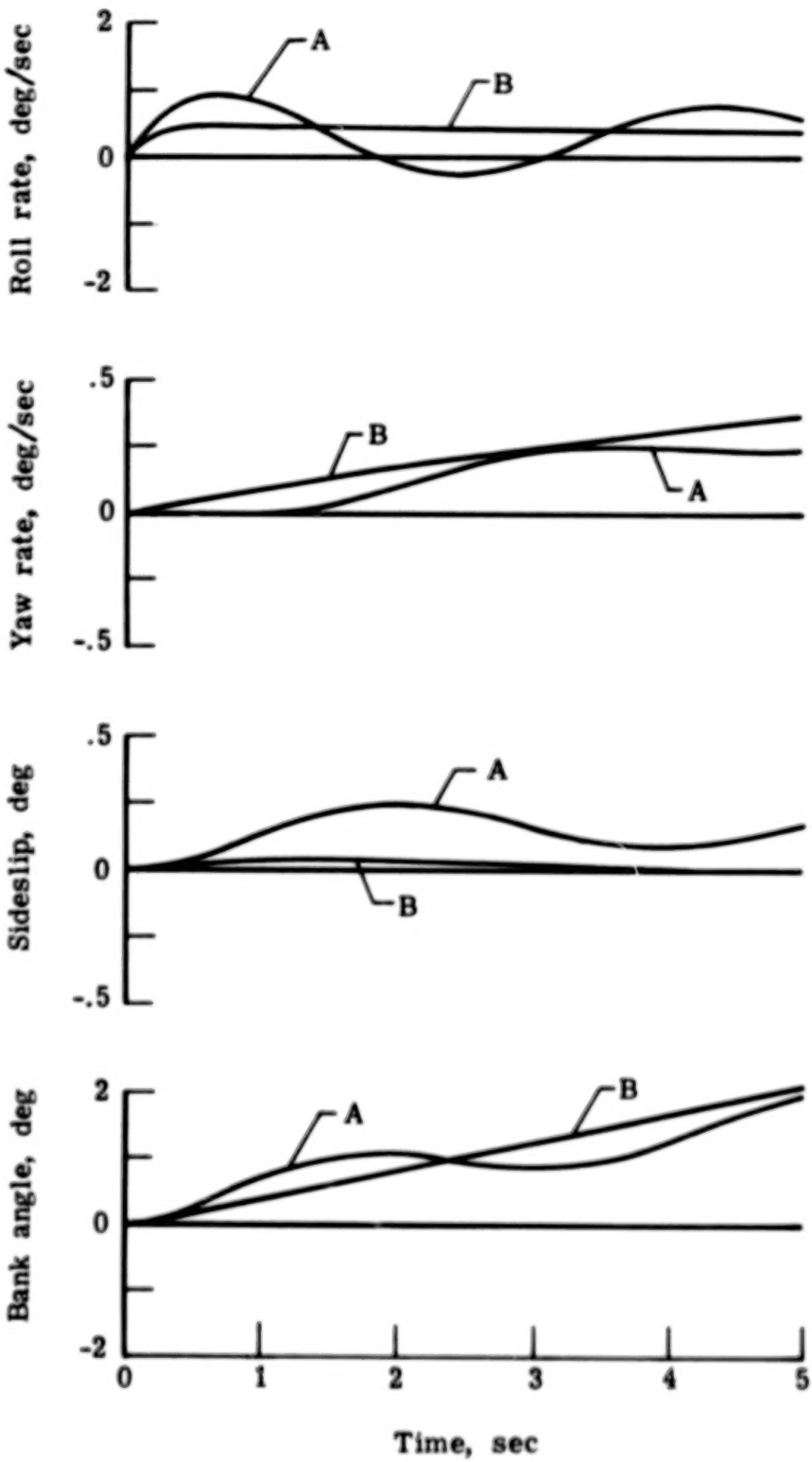

(b) Flight condition 17 (landing approach).

Figure 2.- Continued.

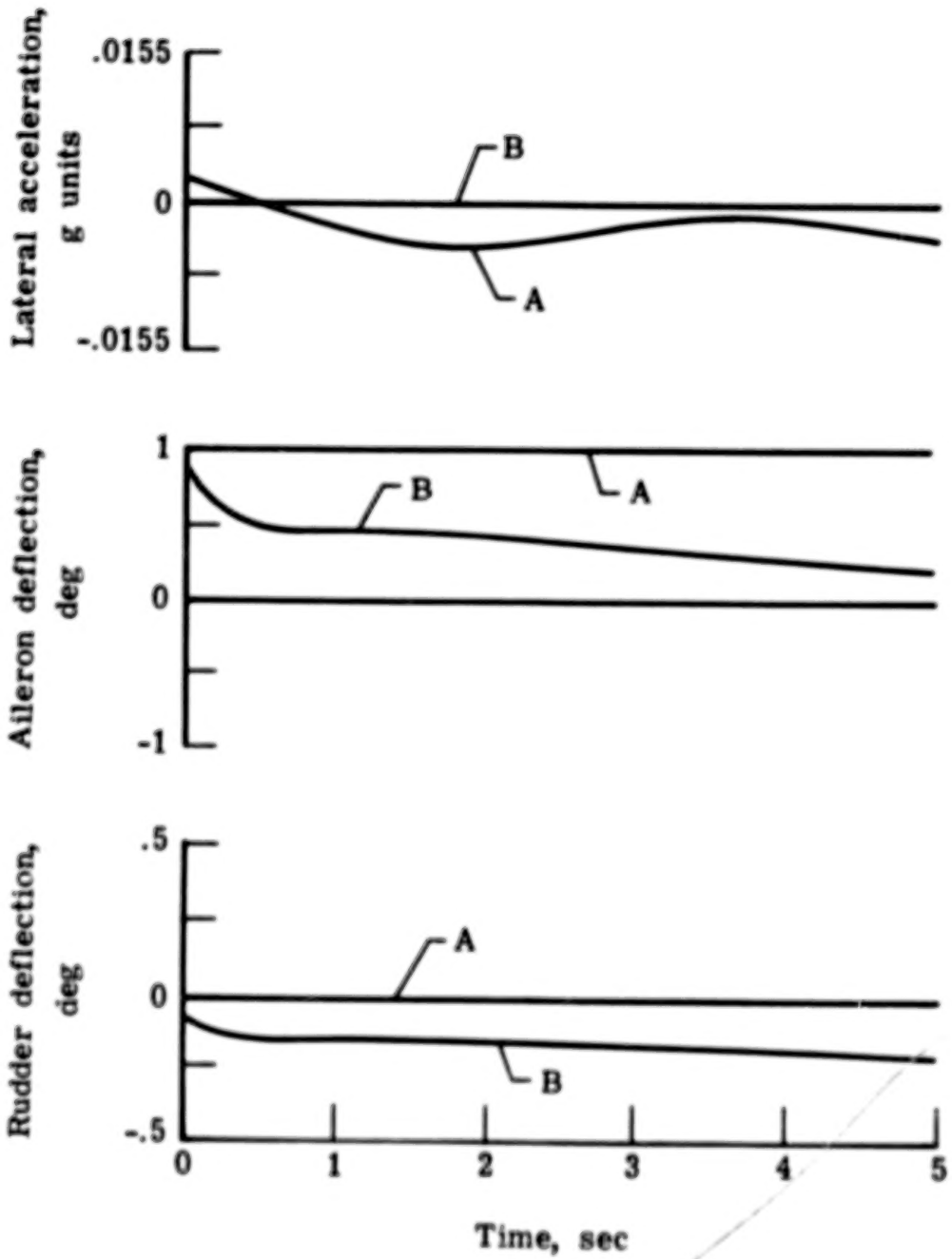

(b) Concluded.

Figure 2.- Continued.

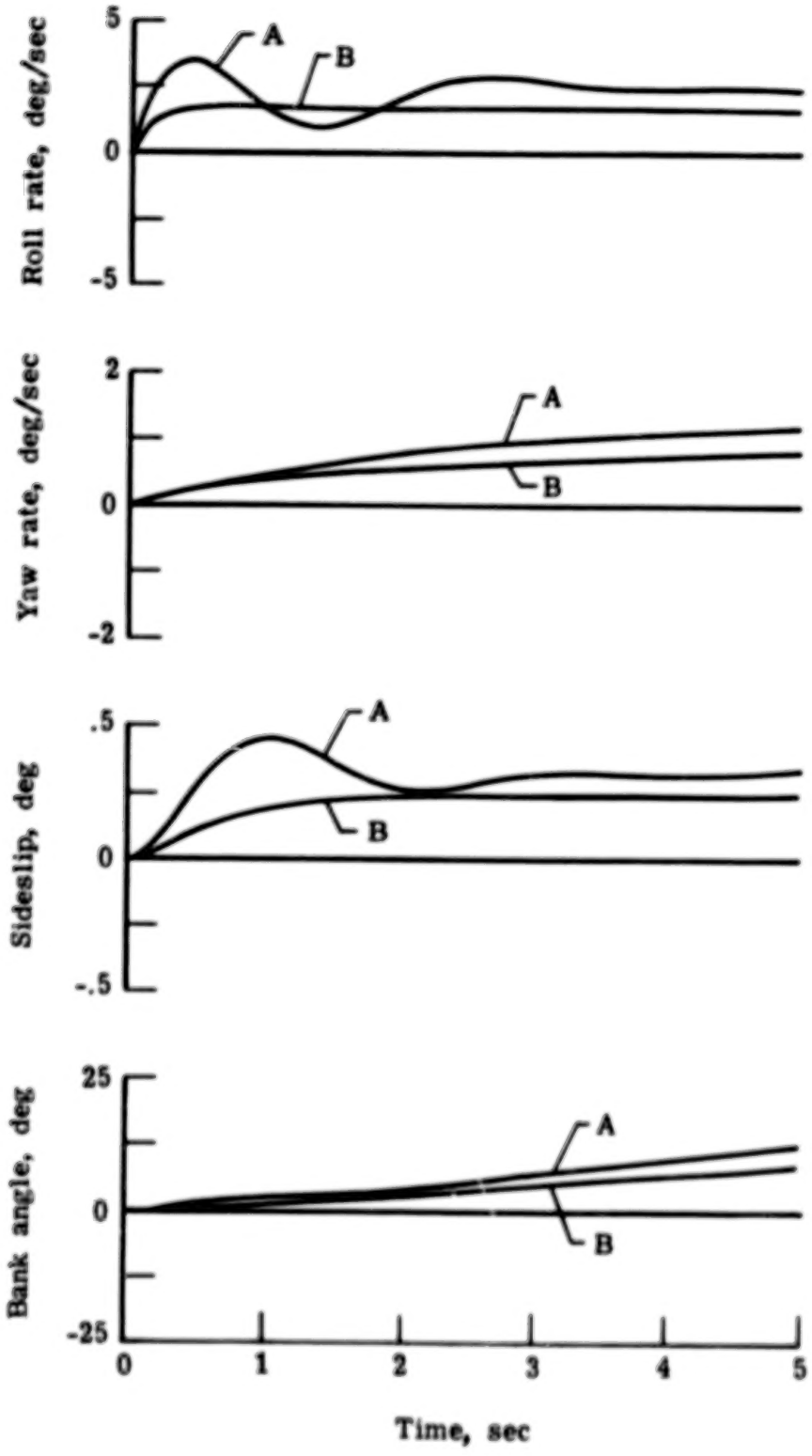

(c) Flight condition 20 (high angle of attack).

Figure 2.- Continued.

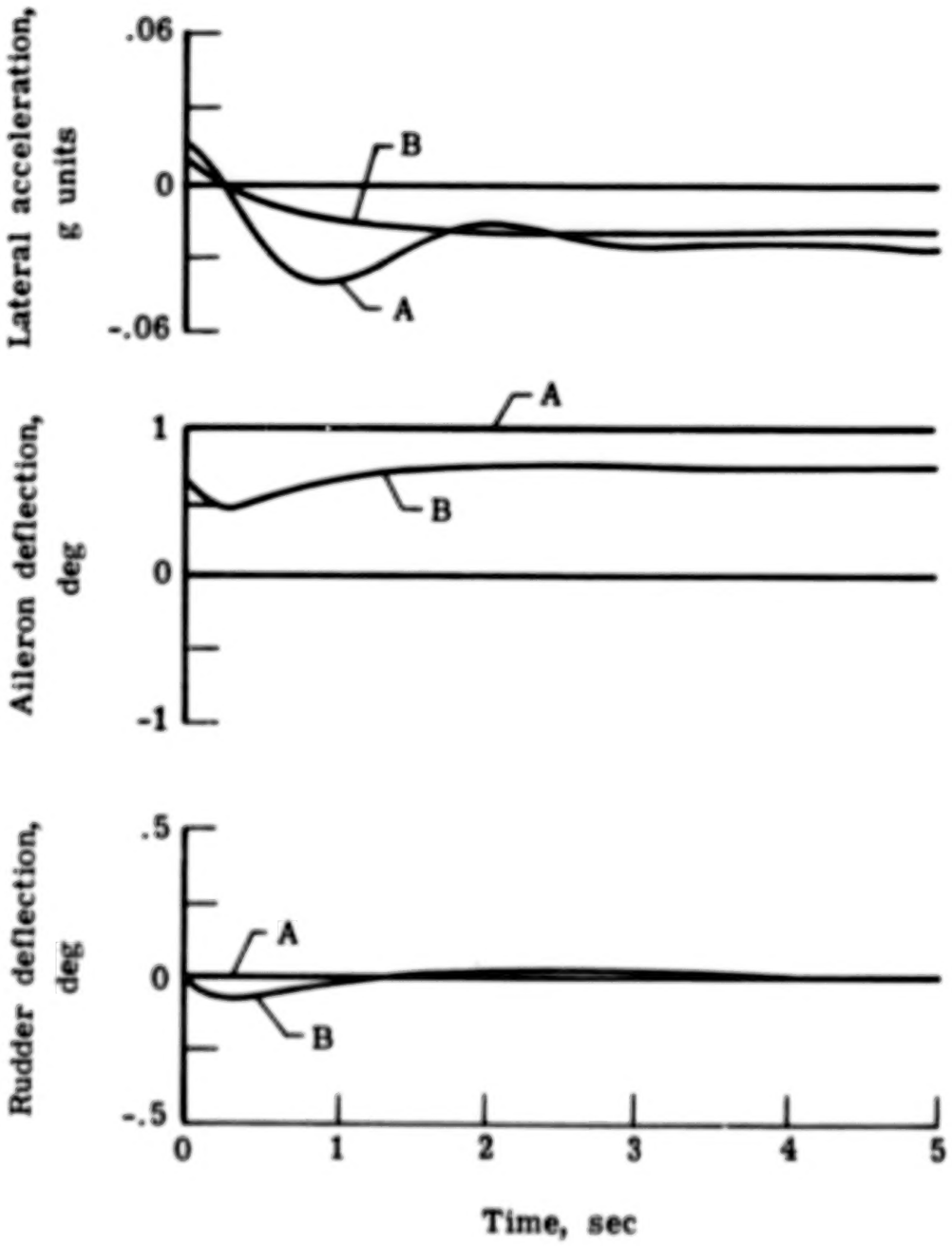

(c) Concluded.

Figure 2.- Concluded.

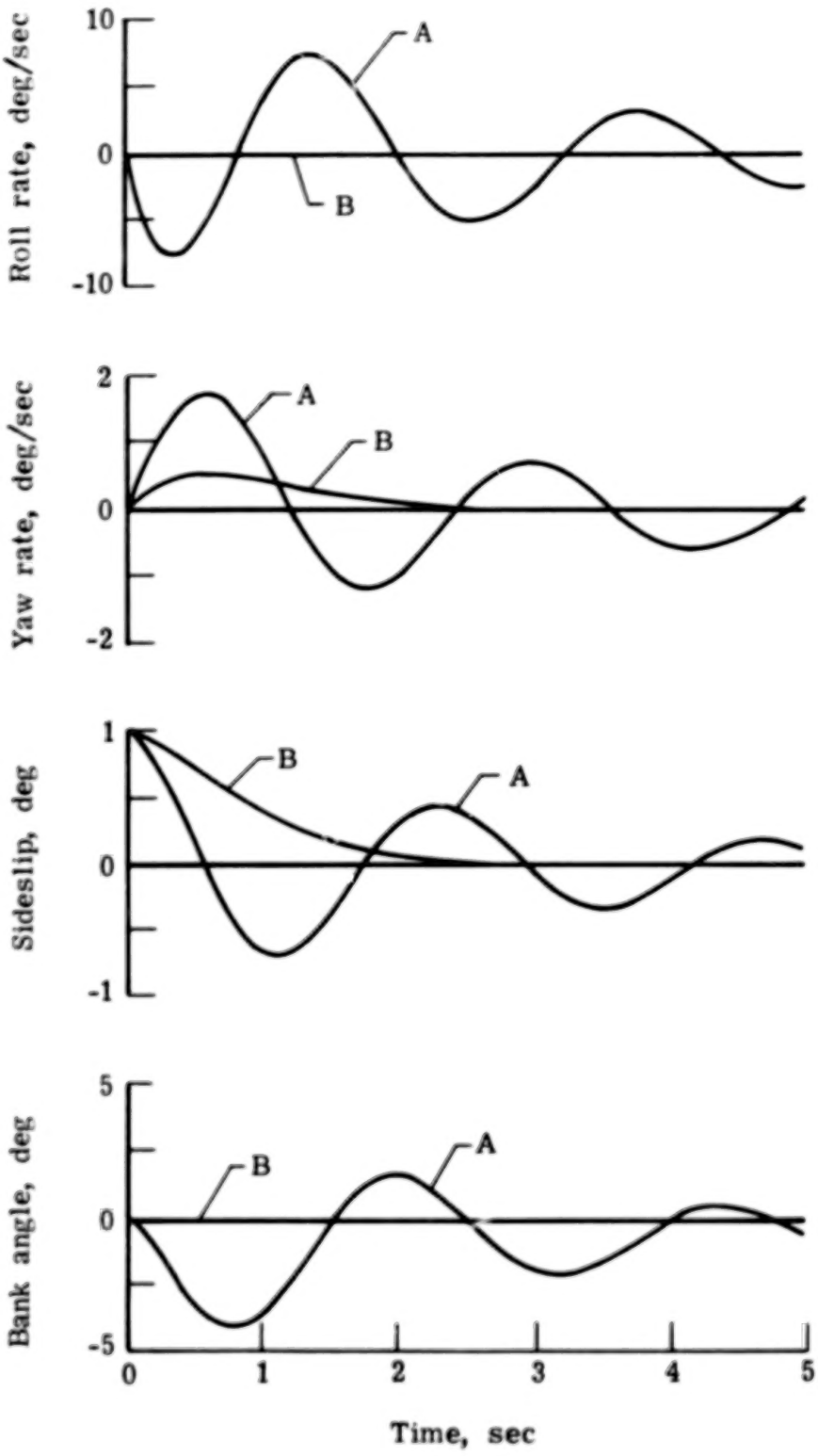

(a) Flight condition 1 (nominal cruise).

Figure 3.- Comparison of free aircraft and augmented aircraft response to sideslip step disturbances. $\beta(0) = 1^{\circ}$. A indicates free aircraft response and B corresponds to augmented aircraft response.

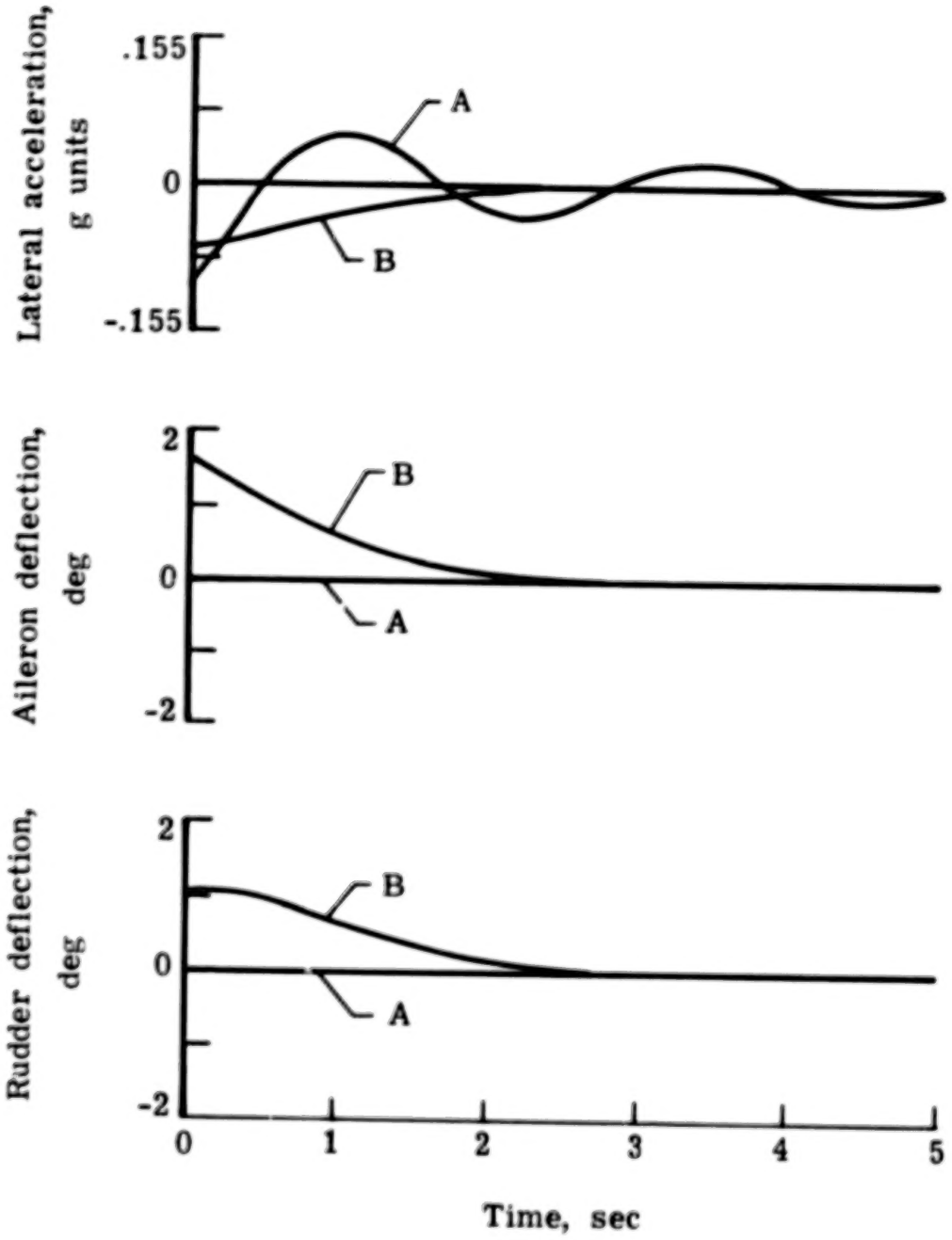

(a) Concluded.

Figure 3.- Continued.

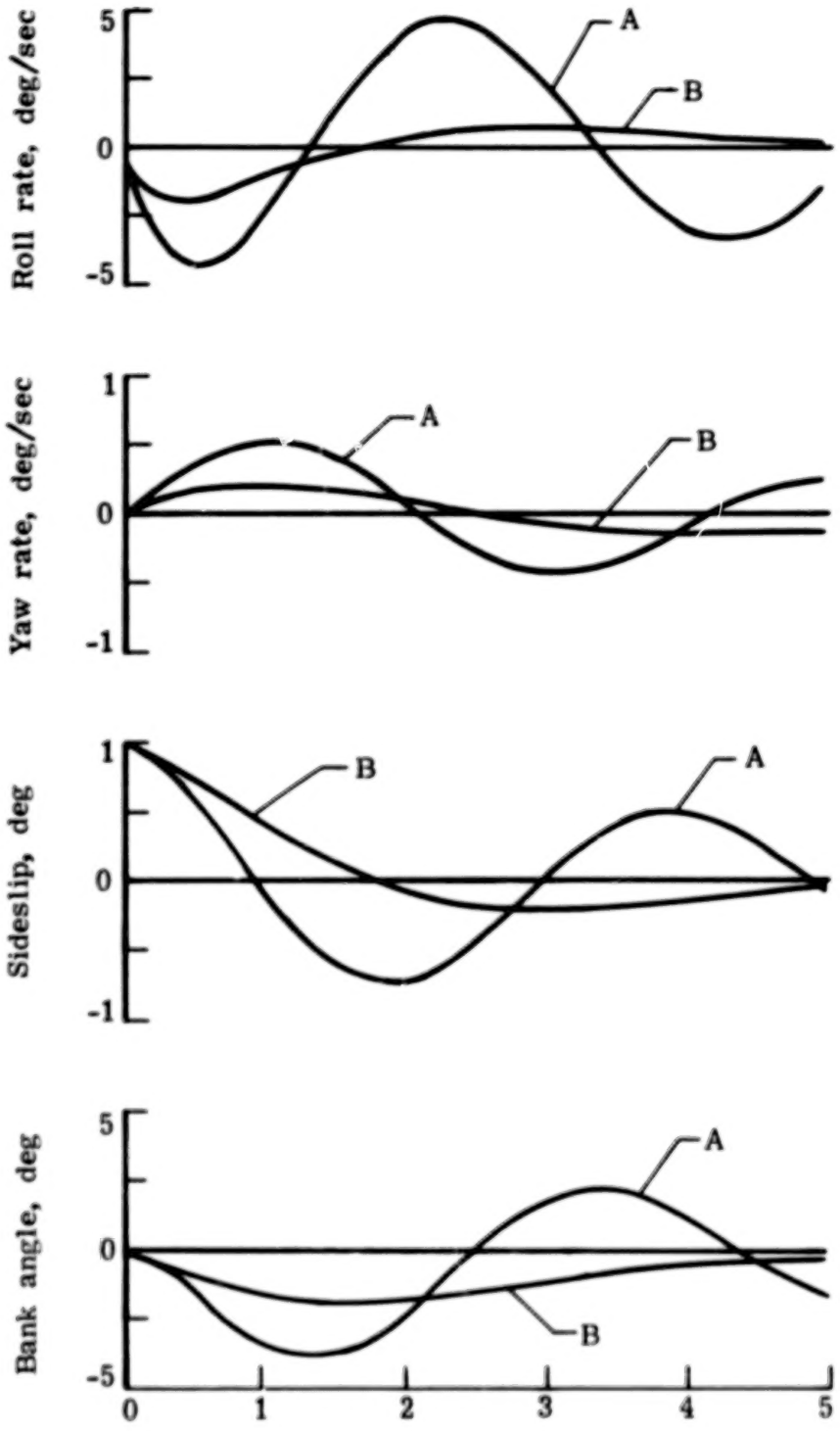

(b) Flight condition 17 (landing approach).

Figure 3.- Continued.

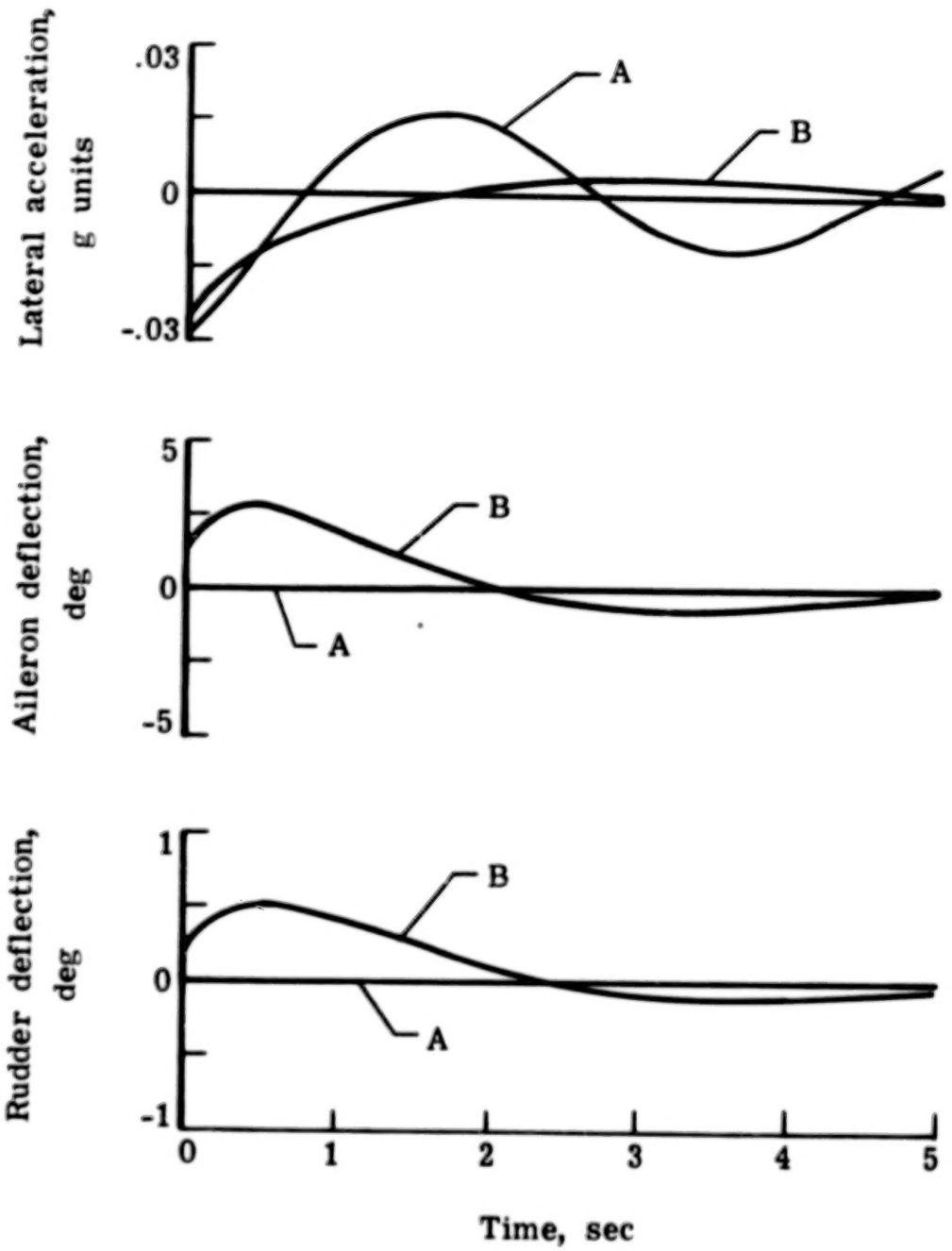

(b) Concluded.

Figure 3.- Continued.

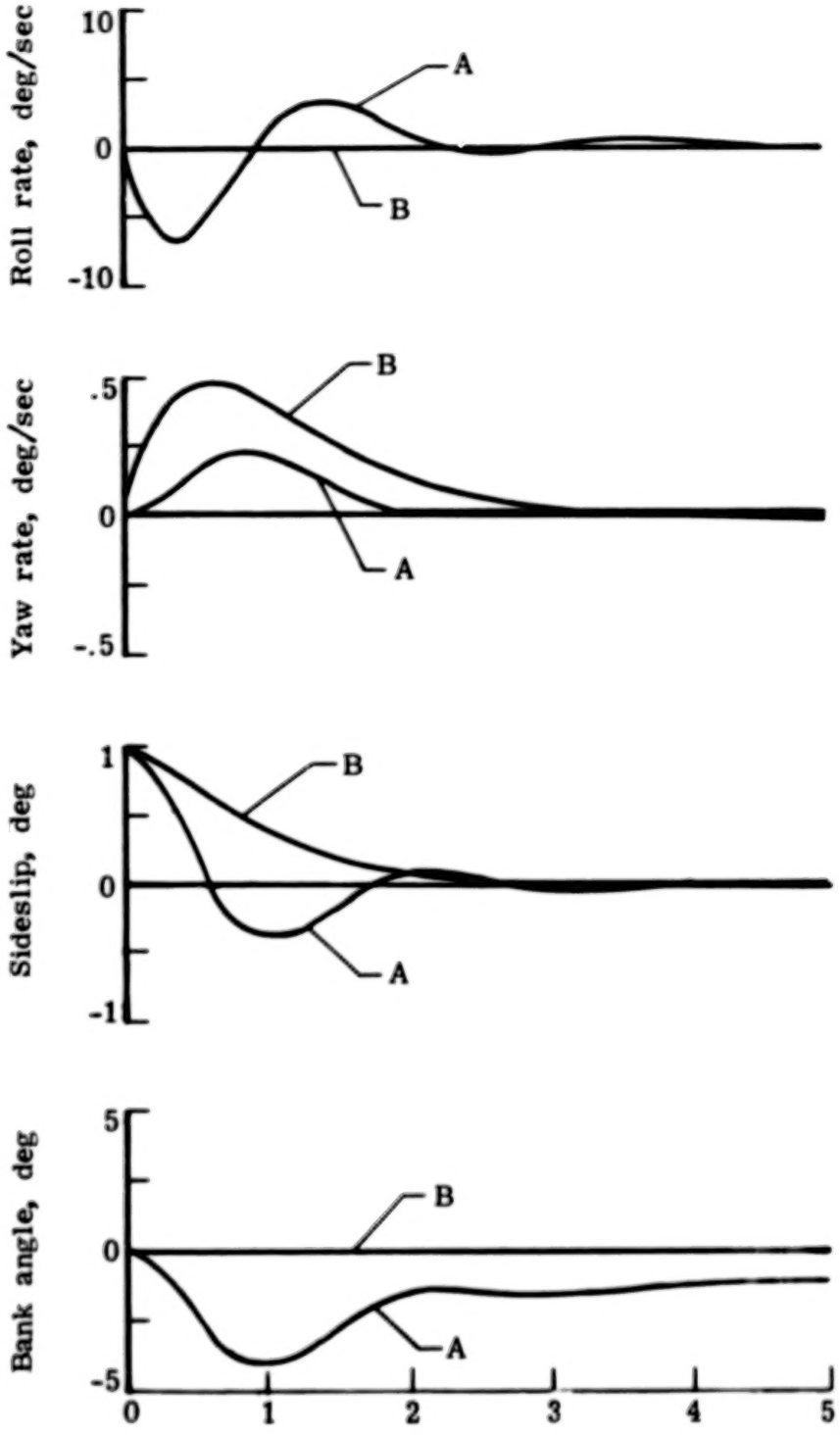

(c) Flight condition 20 (high angle of attack).

Figure 3.- Continued.

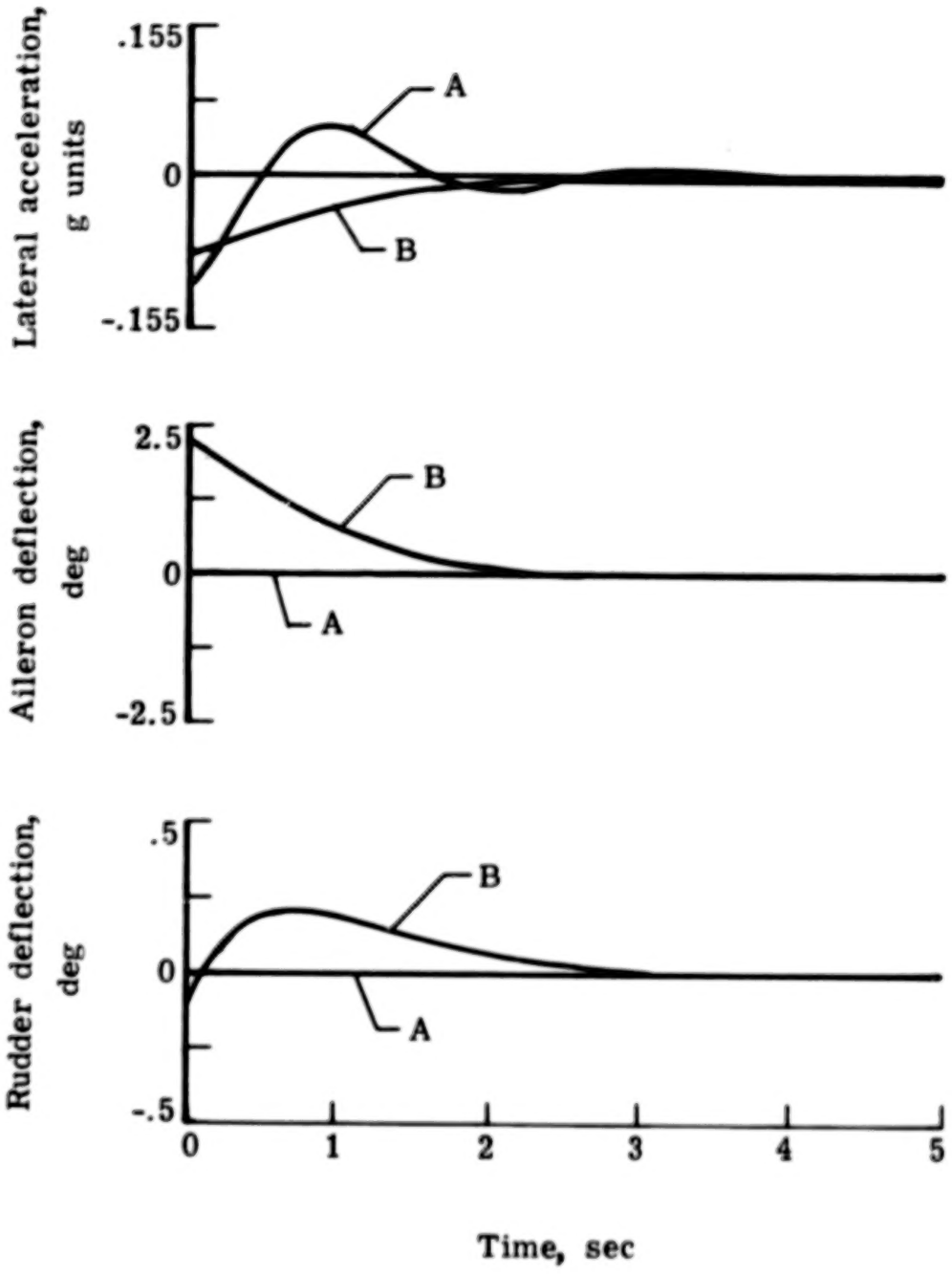

(c) Concluded.

Figure 3.- Concluded.

1. Report No.	2. Government Accession No.	3. Recipient's Catalog No.
NASA TP-1234		

4. Title and Subtitle	5. Report Date
MODAL CONTROL THEORY AND APPLICATION TO AIRCRAFT LATERAL HANDLING QUALITIES DESIGN	June 1978
	6. Performing Organization Code
7. Author(s)	8. Performing Organization Report No.
S. Srinathkumar	L-12177
	10. Work Unit No.
9. Performing Organization Name and Address	505-07-33-04
NASA Langley Research Center Hampton, VA 23665	11. Contract or Grant No.
	13. Type of Report and Period Covered
12. Sponsoring Agency Name and Address	Technical Paper
National Aeronautics and Space Administration Washington, DC 20546	14. Sponsoring Agency Code

15. Supplementary Notes

S. Srinathkumar: NASA-NRC Associate, Langley Research Center.

16. Abstract

A multivariable synthesis procedure based on eigenvalue/eigenvector assignment is reviewed and is employed to develop a systematic design procedure to meet the lateral handling qualities design objectives of a fighter aircraft over a wide range of flight conditions. The study reveals that the closed-loop modal characterization developed provides significant insight into the design process and plays a pivotal role in the synthesis of robust feedback systems. The simplicity of the synthesis algorithm yields an efficient computer-aided interactive design tool for flight control system synthesis.

17. Key Words (Suggested by Author(s))	18. Distribution Statement
Eigenvalues Eigenvectors Modal control Aircraft control systems Handling qualities	Unclassified - Unlimited Subject Category 08

19. Security Classif. (of this report)	20. Security Classif. (of this page)	21. No. of Pages	22. Price*
Unclassified	Unclassified	60	$5.25

* For sale by the National Technical Information Service, Springfield, Virginia 22161

NASA-Langley, 1978

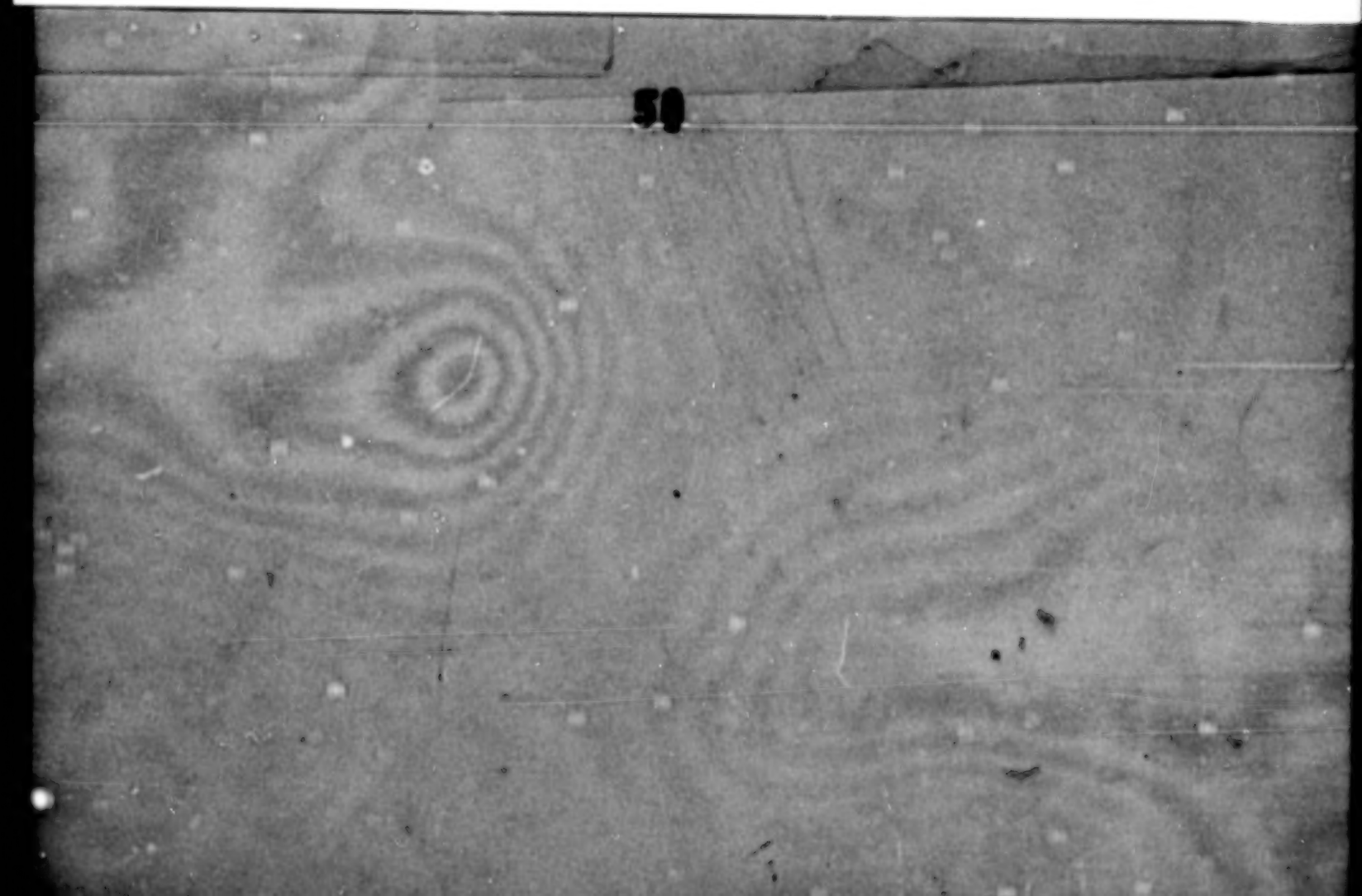
50